AMERICAN SOCIETY FOR MICROBIOLOGY | Journal of Virology®

VIRUS-CELL INTERACTIONS

Functional and Physical Interaction between the Arf Activator GBF1 and Hepatitis C Virus NS3 Protein

Nadjet Lebsir,[a] Lucie Goueslain,[b] Rayan Farhat,[a]* Nathalie Callens,[a] Jean Dubuisson,[a] Catherine L. Jackson,[b] Yves Rouillé[a]

[a]University of Lille, CNRS, Inserm, CHU Lille, Institut Pasteur de Lille, U1019-UMR 8204-CIIL-Centre d'Infection et d'Immunité de Lille, Lille, France
[b]Institut Jacques Monod, UMR 7592 CNRS, Université Paris Diderot-Paris 7, Paris, France

ABSTRACT GBF1 has emerged as a host factor required for the genome replication of RNA viruses of different families. During the hepatitis C virus (HCV) life cycle, GBF1 performs a critical function at the onset of genome replication but is dispensable when the replication is established. To better understand how GBF1 regulates HCV infection, we have looked for interactions between GBF1 and HCV proteins. NS3 was found to interact with GBF1 in yeast two-hybrid, coimmunoprecipitation, and proximity ligation assays and to interfere with GBF1 function and alter GBF1 intracellular localization in cells expressing NS3. The interaction was mapped to the Sec7 domain of GBF1 and the protease domain of NS3. A reverse yeast two-hybrid screen to identify mutations altering NS3-GBF1 interaction yielded an NS3 mutant (N77D, Con1 strain) that is nonreplicative despite conserved protease activity and does not interact with GBF1. The mutated residue is exposed at the surface of NS3, suggesting it is part of the domain of NS3 that interacts with GBF1. The corresponding mutation in strain JFH-1 (S77D) produces a similar phenotype. Our results provide evidence for an interaction between NS3 and GBF1 and suggest that an alteration of this interaction is detrimental to HCV genome replication.

IMPORTANCE Single-stranded, positive-sense RNA viruses rely to a significant extent on host factors to achieve the replication of their genome. GBF1 is such a cellular protein that is required for the replication of several RNA viruses, but its mechanism of action during viral infections is not yet defined. In this study, we investigated potential interactions that GBF1 might engage in with proteins of HCV, a GBF1-dependent virus. We found that GBF1 interacts with NS3, a nonstructural protein involved in HCV genome replication, and our results suggest that this interaction is important for GBF1 function during HCV replication. Interestingly, GBF1 interaction with HCV appears different from its interaction with enteroviruses, another group of GBF1-dependent RNA viruses, in keeping with the fact that HCV and enteroviruses use different functions of GBF1.

KEYWORDS ADP ribosylation factor, GBF1, NS3, hepatitis C virus, viral replication

Hepatitis C virus (HCV) is a small, enveloped, single-stranded, positive-sense RNA virus that infects human hepatocytes and causes persistent infection in most HCV patients. HCV replicates its genome in the cytoplasm of the host cell. Its RNA-dependent RNA polymerase and other nonstructural proteins implicated in genome replication are found in association with rearranged cellular membranes, which have been named the membranous web (1). The membranous web is composed of single membrane and double membrane vesicles (2, 3) originating from the endoplasmic reticulum (ER) membrane. Two viral proteins, NS4B and NS5A, appear to play a major role in the induction of membrane rearrangements (3, 4). The protease and helicase NS3-4A and the RNA-dependent RNA polymerase NS5B are also included in HCV replication complexes, in addition to NS4B and NS5A. Cell host factors from the ER such as VAP-A (5) and phosphatidylinositol-4-kinase alpha (PI4KIIIα) (6–10) are recruited to

Citation Lebsir N, Goueslain L, Farhat R, Callens N, Dubuisson J, Jackson CL, Rouillé Y. 2019. Functional and physical interaction between the Arf activator GBF1 and hepatitis C virus NS3 protein. J Virol 93:e01459-18. https://doi.org/10.1128/JVI.01459-18.

Editor J.-H. James Ou, University of Southern California

Copyright © 2019 American Society for Microbiology. All Rights Reserved.

Address correspondence to Catherine L. Jackson, cathy.jackson@ijm.fr, or Yves Rouillé, yves.rouille@ibl.cnrs.fr.

* Present address: Rayan Farhat, Inserm U1052, Cancer Research Center of Lyon (CRCL), Université de Lyon (UCBL1), CNRS UMR-5286, Centre Léon Bérard, Lyon, France.

N.L. and L.G. contributed equally to the study.

Received 23 August 2018
Accepted 14 December 2018
Accepted manuscript posted online 19 December 2018
Published 5 March 2019

the membranous web and are functionally involved in HCV genome replication. In addition, cellular factors from other cellular compartments, including Rab5 (11), OSBP (12), and FAPP2 (13), are also recruited to the membranous web and play essential functions in viral RNA replication. Interactions with NS5A appear to play important roles in the recruitment of most of these cellular factors.

We previously identified GBF1 as a host factor critical for HCV genome replication (14). GBF1 is a brefeldin A (BFA)-sensitive guanine nucleotide exchange factor (GEF) that activates Arf family members (15). Through Arf1 activation, it participates in the regulation of COPI-dependent vesicular transport, phospholipid metabolism, actin cytoskeleton dynamics at the Golgi membrane, and lipid droplet metabolism (16, 17). Its inhibition by BFA or golgicide A (GCA) leads to inhibition of secretion and disassembly of the Golgi complex. GBF1 has six conserved domains (18). Its Arf-GEF activity is catalyzed by the Sec7 domain and is selective for class I Arfs (Arf1-3) and class II Arfs (Arf4 and Arf5) (15, 19). The functions of the other conserved domains are less well defined (18, 20). In addition to HCV, GBF1 is a host factor involved in the replication of RNA viruses of the families *Picornaviridae* (21–23), *Coronaviridae* (24), *Flaviviridae* (25), and *Hepeviridae* (26).

Little is known about the mechanism of action of GBF1 in HCV and other viral infections. Its Arf-GEF activity appears to be of special importance at the onset of HCV genome replication but is not essential when the replication is established (14). However, its Arf-GEF activity is not required for the formation of membrane rearrangements leading to the formation of the membranous web (14), suggesting rather that GBF1 is involved in a postformation step of membrane-associated replication complex function. It has been proposed that GBF1 is involved in the generation of phosphatidylinositol-4-phosphate (PI4P)-enriched replication complexes through Arf1-dependent activation of Golgi-resident PI4 kinase-IIIβ (27). However, the involvement of this kinase during HCV genome replication is still controversial (28–32). Moreover, we recently demonstrated that the function of GBF1 during HCV genome replication is not mediated by Arf1 and is distinct from its regulatory functions with respect to the cellular secretory pathway and the morphology of the Golgi complex (33). GBF1 function in HCV replication is mediated by the pair Arf4 and Arf5, whereas its function in the regulation of the secretory pathway is mediated by the pair Arf1 and Arf4 (33, 34). The involvement of class II Arfs in viral replication appears to be conserved for some, but not all, RNA viruses (35). To obtain more insight into how GBF1 regulates HCV genome replication, we investigated in this study potential interactions between GBF1 and HCV proteins.

RESULTS

NS3 interacts with GBF1. Potential interactions between HCV proteins and GBF1 were investigated using a yeast two-hybrid assay. The HCV proteins core, E1, E2, p7, NS2, NS3, NS4A, NS4B, NS5A, and NS5B were each tested individually for interaction with GBF1. In addition to GBF1, there are two other Golgi-localized Arf GEFs, BIG1 and BIG2, which are not required for HCV infection. To test potential specificity in interaction, BIG1 and BIG2 were each tested, in addition to GBF1, for interaction with HCV proteins. Because of the large size of the Arf GEFs, three domains of each GEF protein were tested individually: the N terminus, the catalytic Sec7 domain, and the C terminus. Among the 90 combinations tested, only one interaction was found, between NS3 and the catalytic Sec7 domain of GBF1 (Fig. 1A). No interaction was observed with any other HCV protein, and only the Sec7 domain of GBF1 among the Arf GEFs tested gave a positive signal (see the data set in the supplemental material).

Deletion mutants were used to further map the interaction within NS3. We found an interaction between the Sec7 domain of GBF1 and the protease domain of NS3 (Fig. 1A). The interaction between the Sec7 domain of GBF1 and the protease domain of NS3 was observed with strains Con1, H77, and JFH-1 (Fig. 1A), indicating a conservation of this interaction for the three strains tested but with some difference concerning the strength of the interaction.

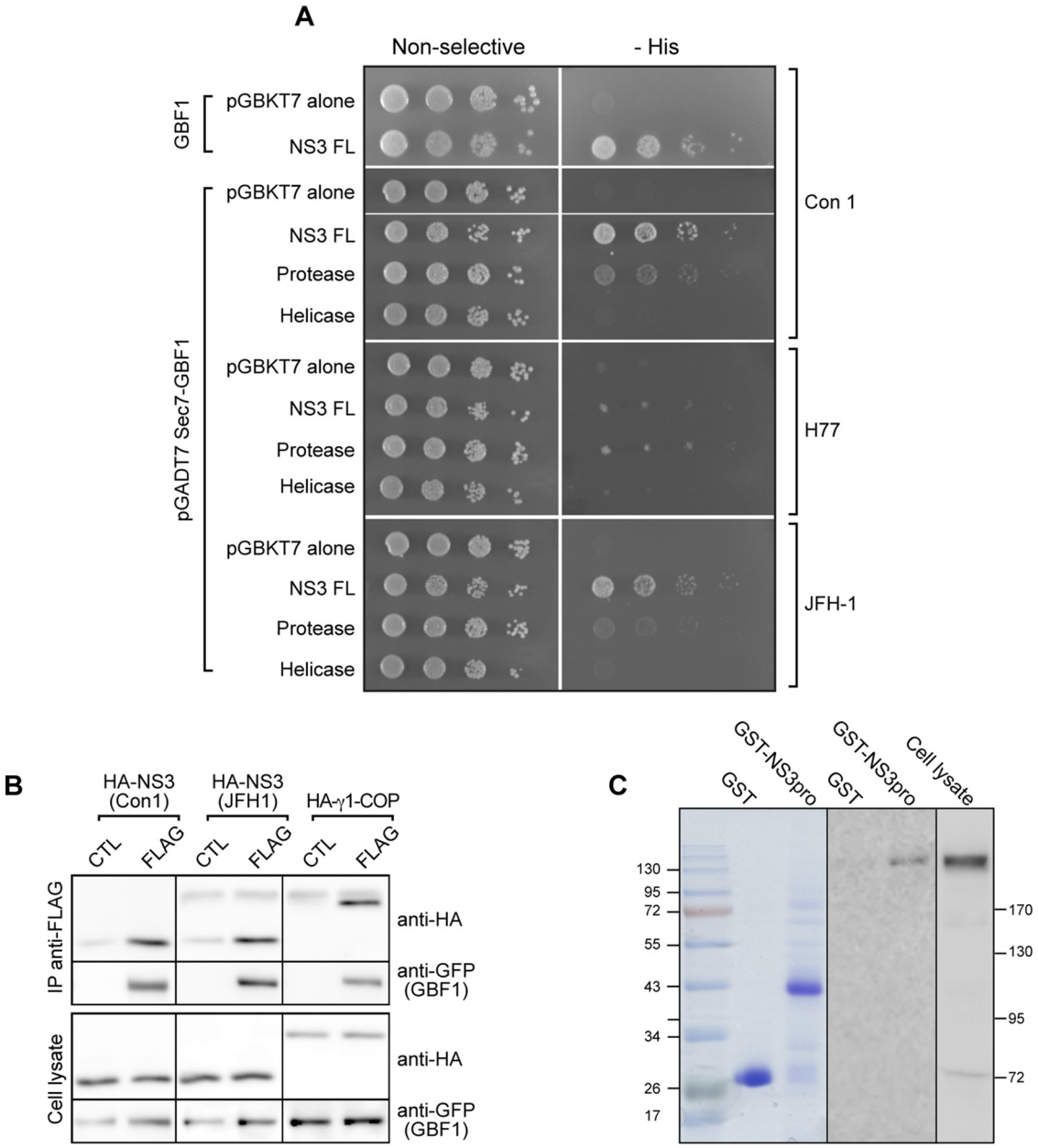

FIG 1 NS3 interacts with GBF1. (A) pGBKT7 plasmids carrying full-length NS3 (Con1 strain), the indicated fragments from the Con1, H77, and JFH1 strains, or pGBKT7 alone were cotransformed into yeast strain AH109 with the pGADT7 plasmids carrying full-length GBF1 (GBF1) or the catalytic Sec7 domain as indicated. Transformants were plated onto nonselective medium (left) or onto plates lacking histidine (−His) to monitor expression of the reporter His3 (right). Tenfold serial dilutions of each culture were spotted from left to right for each transformed strain. (B) HA-tagged NS3-4A of Con1 or JFH-1 or HA-tagged γ1-COP was coexpressed with YFP-GBF1 (CTL) or YFP-GBF1-FLAG (FLAG) in HeLa cells. Cells were lysed and lysates precipitated with anti-FLAG beads. Immunoprecipitated material and 5% of lysates were analyzed by immunoblotting with anti-HA and anti-GFP antibodies. (C) GST fused to the NS3 protease domain (GST-pro) or GST (left) were coupled to glutathione-Sepharose beads and incubated with 400 μl of HeLa cell cytoplasmic lysate. (Right) The lysate (10 μl) and the material bound to beads were analyzed by immunoblotting with an anti-GBF1 antibody.

To confirm this interaction, we used next a coimmunoprecipitation (co-IP) assay. A hemagglutinin (HA)-tagged version of NS3-4A from the Con1 or JFH-1 strain was coexpressed with a FLAG-tagged version of YFP-GBF1 in HeLa cells and immunoprecipitated with an anti-FLAG antibody. As a control, we used an HA-tagged version of human γ1-COP, a COPI subunit previously shown to interact with GBF1 (36). Under control conditions, a band of low intensity was observed with NS3 but not γ1-COP, probably corresponding to nonspecific binding of HA-NS3 to the beads. The intensity

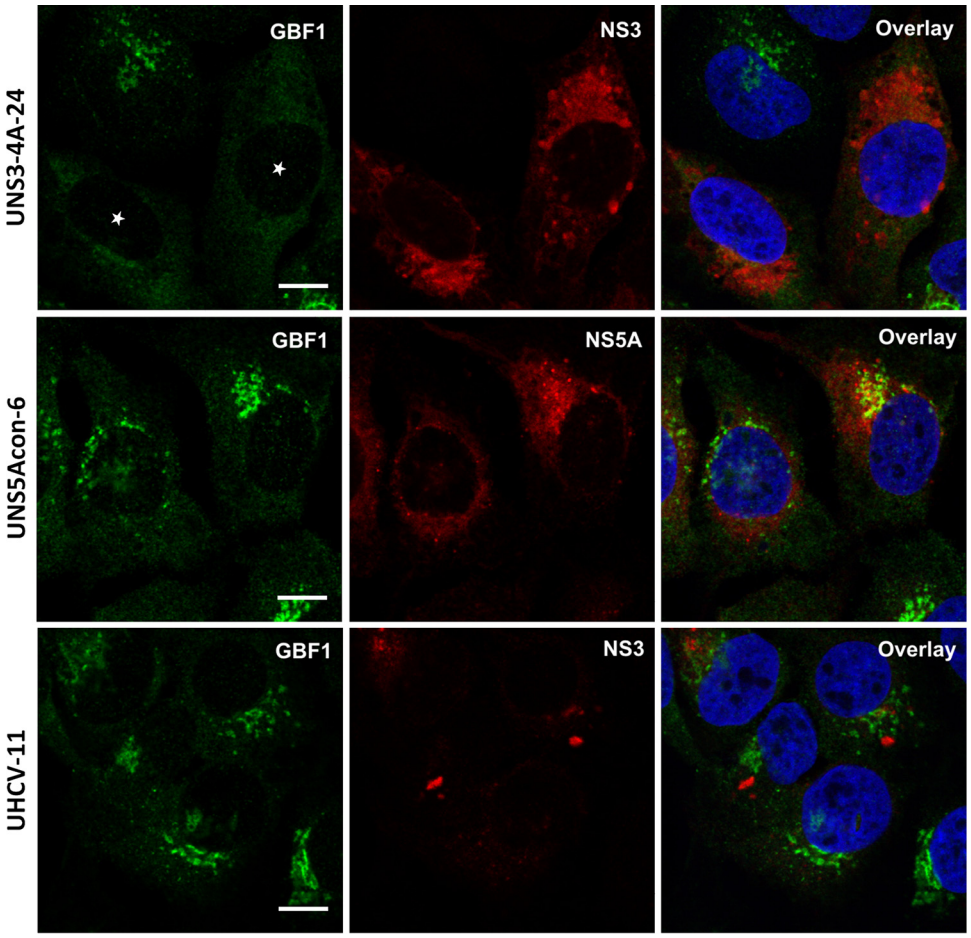

FIG 2 GBF1 localization is altered in cells expressing HCV NS3-4A. UNS3-4A-24, UNS5Acon-6, and UHCV-11 cells were induced for 24 h and processed for immunofluorescence detection of GBF1 (green) and NS3 or NS5A (red), as indicated. White stars indicate cells expressing NS3. Bars, 10 μm.

of the coimmunoprecipitated NS3 bands was much stronger than the background observed under control conditions (Fig. 1B). These results indicated that NS3, like the positive-control γ1-COP, interacted with GBF1 in this assay.

The interaction was further investigated with a pulldown assay using glutathione *S*-transferase (GST) fused to the protease domain of NS3 from the Con1 strain (GST-pro). A HeLa cell lysate was incubated with GST-pro, or GST as a control, coupled to glutathione-Sepharose beads. The material bound to the beads was analyzed by immunoblotting using an anti-GBF1 antibody. A band corresponding to GBF1 was observed with the GST-pro construct but not with GST (Fig. 1C). This result confirmed the capacity of GBF1 to interact with the protease domain of NS3.

GBF1 localization is altered in cells overexpressing NS3-4A. To assess the impact of NS3 on GBF1 intracellular localization, we made use of U-2 OS cells with inducible expression of green fluorescent protein (GFP) (UGFP-9.22) (37), of NS3/4A (UNS3-4A-24) (38), of NS5A (UNS5Acon-6) (39), or of the entire HCV polyprotein (UHCV-11) (40). As expected in control noninduced cells, GBF1 had a Golgi-like localization and a less intense cytosolic localization (data not shown). In induced cells, the distribution of GBF1 to the Golgi membrane and cytosol appeared identical to control conditions in cells expressing GFP (data not shown), NS5A, or the polyprotein (Fig. 2). In contrast, the Golgi-like localization of GBF1 was not observed in UNS3-4A-24 cells expressing NS3-4A (Fig. 2). A partial colocalization of NS3 and GBF1 was measured in induced UNS3-4A-24 cells expressing NS3-4A alone but not in induced UHCV-11 cells expressing the polyprotein (Fig. 3A). Immunoblot analysis of GBF1 in UNS3-4A-24 cells revealed a

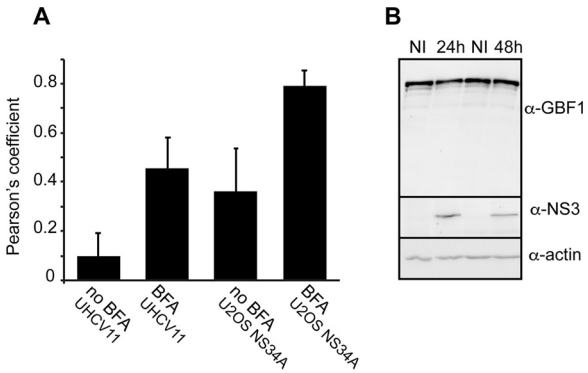

FIG 3 Quantification of GBF1-NS3 colocalization and GBF1 expression in cells expressing NS3. (A) The colocalization of NS3 and GBF1 in UNS3-4A-24 and UHCV-11 cells induced for 24 h and treated with 10 μg/ml BFA for 30 min or left untreated was quantified by calculating the Pearson's correlation coefficient of at least 10 cells. Error bars represent the standard deviations (SD). (B) The expression of NS3 was induced in UNS3-4A-24 cells for 24 or 48 h. The cells were lysed and GBF1, NS3, and actin expression was analyzed by immunoblotting. NI, not induced.

similar level of expression of GBF1 under induced and noninduced conditions (Fig. 3B), indicating that the loss of the Golgi localization did not result from GBF1 degradation but rather from a change of intracellular localization induced by NS3-4A expression.

We next analyzed the intracellular localization of GBF1 and NS3 in cells treated with GBF1 inhibitor BFA or GCA. These inhibitors of GBF1 activity disrupt Golgi structure, causing fusion of the Golgi membrane with the ER (41). In addition, BFA treatment stabilizes GBF1 association with membranes (42). In UNS3-4A-24 cells treated with BFA or GCA, the localization pattern of GBF1 was strikingly different from that of untreated cells. GBF1 was no longer only diffusely distributed throughout the cytoplasm as in uninduced UNS3-4A-24 cells but rather was found additionally in structures in which it colocalized with NS3 (Fig. 4). GBF1 was localized to structures, likely corresponding to the ER-Golgi fused compartment, in cells expressing GFP (data not shown) or NS5A (Fig. 4). In BFA-treated UHCV-11 cells, a mixed pattern of association with ER-Golgi membranes and with NS3-positive structures was observed (Fig. 4). For both UNS3-4A-24 and UHCV-11 cell lines, the colocalization of GBF1 and NS3 was increased in BFA-treated cells (Fig. 3A).

Together, these data indicate that NS3 interacts with GBF1, and that the two proteins colocalize partly in a compartment that is induced by NS3 expression in cells expressing NS3-4A but not the polyprotein. Upon BFA treatment, the morphology of this compartment is altered, and the colocalization of NS3 and GBF1 is increased in both cell lines.

Functional impact of NS3-GBF1 interaction. To assess the impact of NS3 expression on GBF1 activity, we tested the functionality of the secretory pathway in cells expressing NS3. A fixed amount of luciferase from *Gaussia princeps* (GLuc) was coexpressed with increasing amounts of NS3-4A, and the percentage of secreted GLuc was quantified during a 4-h period. As a control, we incubated cells with BFA, an inhibitor of GBF1 activity. A modest (~10%) reduction of GLuc secretion was measured with the highest expression level of NS3, whereas BFA almost completely inhibited GLuc secretion (Fig. 5A). These results indicated that NS3 has a limited impact on GBF1 function in the secretory pathway.

We next investigated the impact of GBF1 on NS3 activity. Since GBF1 interacts with the protease domain, we focused on protease activity. To quantify NS3 protease activity, we used a GFP-IPS construct (43) as a substrate. In this construct, enhanced GFP (EGFP) is fused to the C-terminal sequence of MAVS (mitochondrial antiviral-signaling protein), also known as IPS (interferon-β promoter stimulator protein 1), which contains an NS3 cleavage site. When coexpressed with NS3, a 41-residue C-terminal peptide was

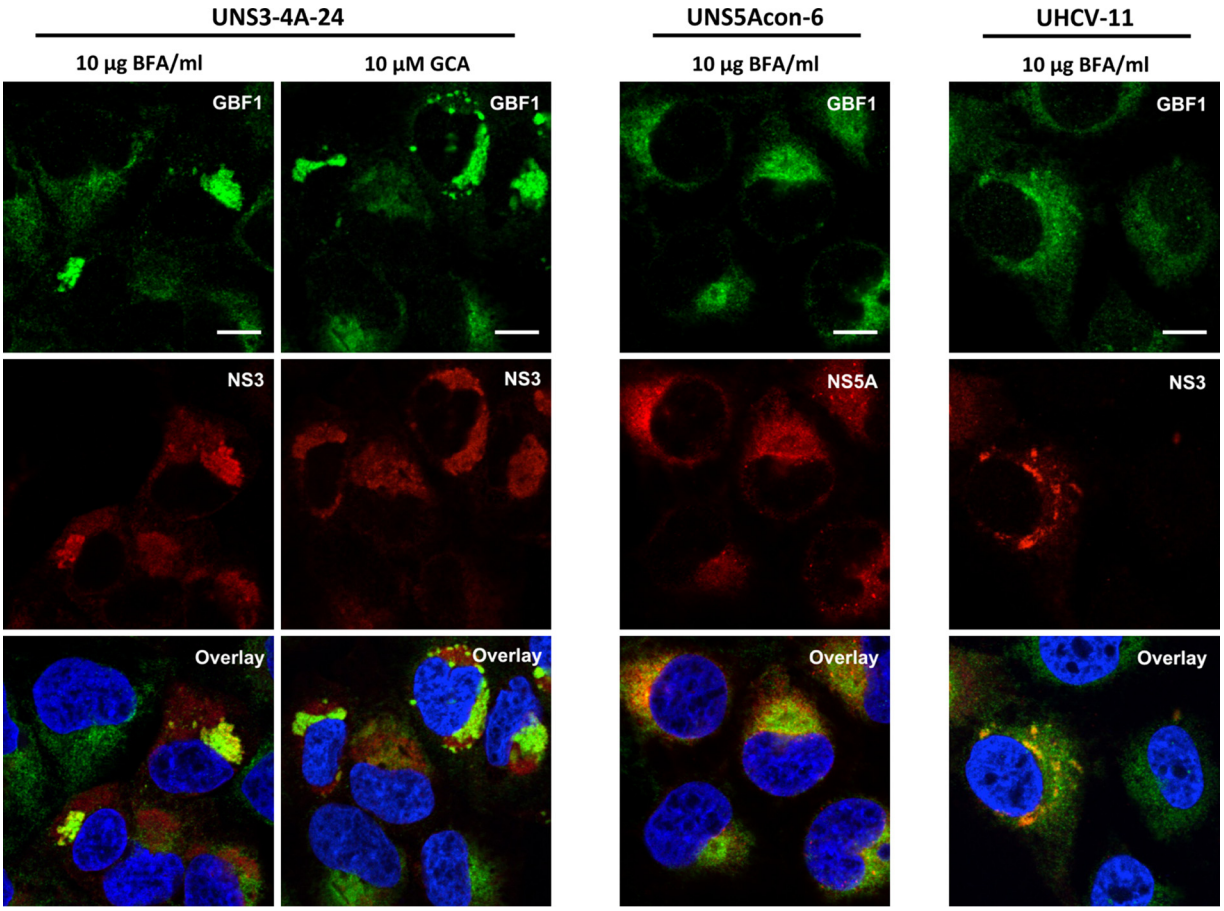

FIG 4 GBF1 colocalizes with HCV NS3 in cells treated with BFA or GCA. UNS3-4A-24, UNS5Acon-6, and UHCV-11 cells were induced for 24 h, treated with BFA or GCA for 30 min, and processed for immunofluorescence detection of GBF1 (green) and NS3 or NS5A (red), as indicated. Bars, 10 μm.

removed from the substrate. This proteolytic cleavage could be visualized by immunoblotting with an anti-GFP antibody (Fig. 5B). When GBF1 was coexpressed with NS3, a dose-dependent reduction of GFP-IPS cleavage was observed (Fig. 5C), yielding up to ~50% inhibition with the highest level of GBF1 expression used in

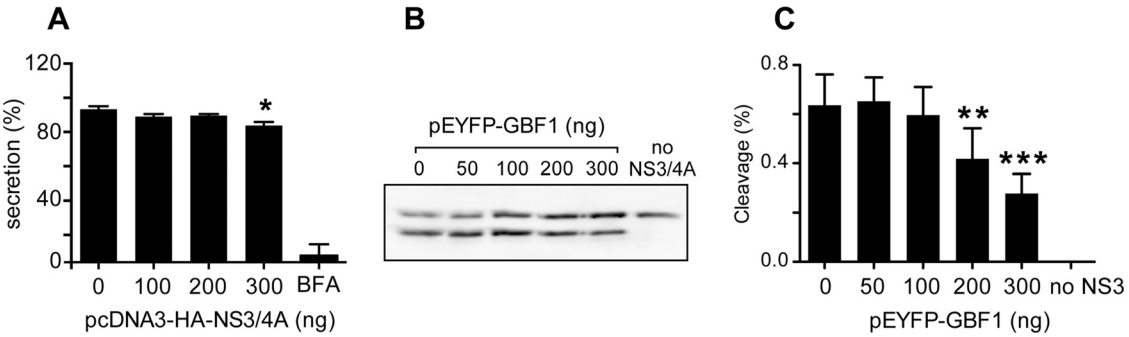

FIG 5 Functional impact of GBF1-NS3 interaction on secretion and NS3 protease activity. (A) HeLa cells were cotransfected with pCMV-GLuc and increasing amounts of pcDNA3.1-HA-NS3-4A as indicated. The total amount of DNA was kept constant by adding empty pcDNA3.1. At 16 h posttransfection, the culture medium was changed and the cells were further incubated for 4 h. As a control, cells were treated with 1 μg/ml BFA during this 4-h secretion period. Luciferase activity was measured in supernatants and cell lysates. (B and C) HeLa cells were cotransfected with pEGFP-IPS, pcDNA3.1 HA-NS3-4A, and increasing concentrations of pEYFP-GBF1 as indicated. Empty pcDNA3.1 plasmid was used to keep the same final concentration of total transfected DNA constant. At 24 h posttransfection, EGFP-IPS cleavage was monitored by immunoblotting using anti-GFP antibody (B), and the intensities of bands corresponding to cleaved and uncleaved GPF-IPS were measured and the percentage of cleavage was calculated (C). Error bars represent the standard deviations for 3 independent experiments. *, **, and *** correspond to *P* values below 0.05, 0.01, and 0.001, respectively.

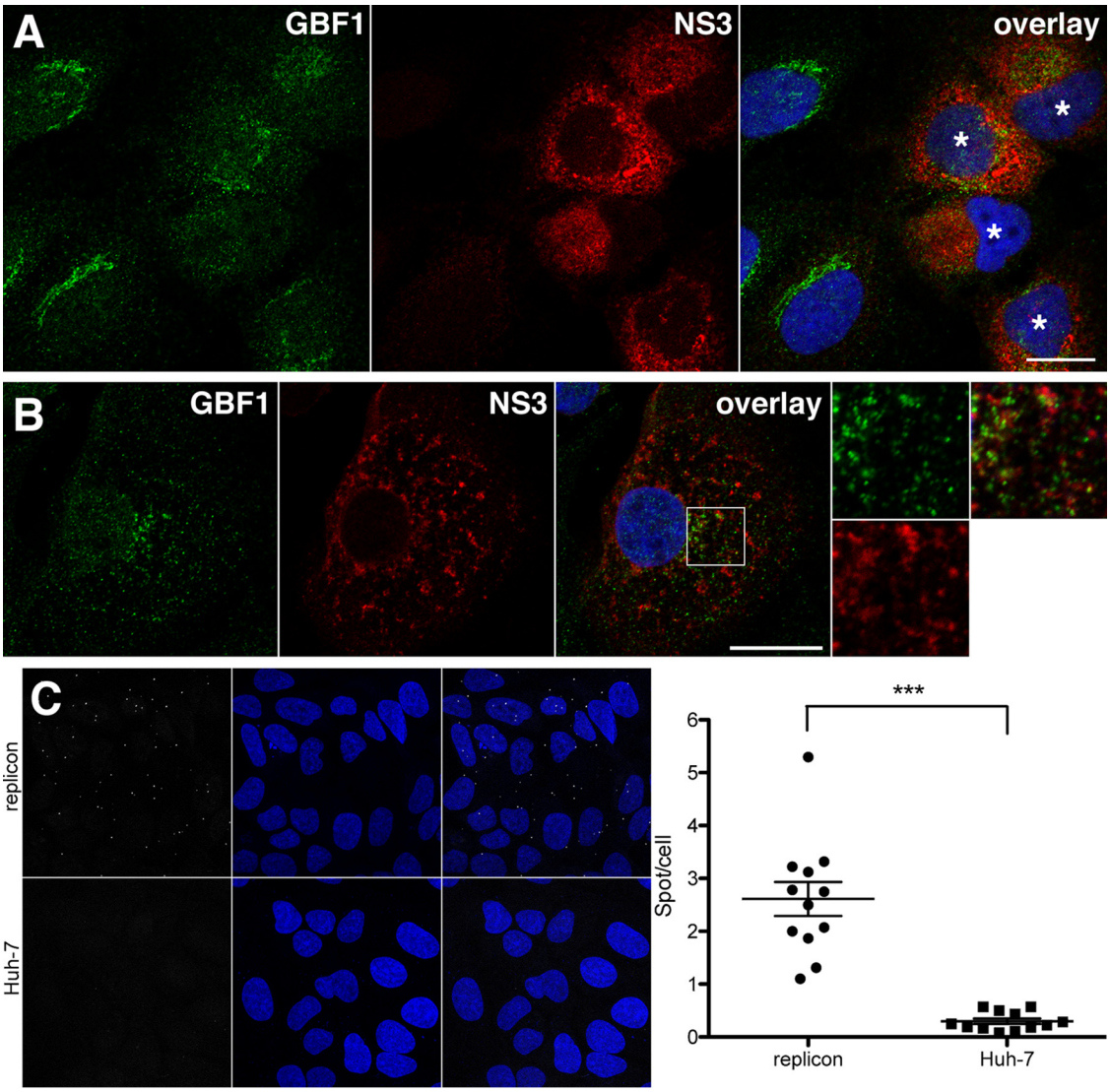

FIG 6 GBF1 interacts with NS3 in cells replicating HCV. (A and B) Huh-7 cells containing a subgenomic replicon of strain JFH-1 were processed for immunofluorescence detection of GBF1 (green) and NS3 (red), as indicated. Note the difference of GBF1 patterns in cells expressing higher levels of NS3 (indicated with a white star in panel A). A higher magnification of the area marked with a square in panel B is shown on the right side. Bars, 20 μm. (C and D) Huh-7 cells containing a subgenomic replicon of JFH-1 strain and naive Huh-7 cells were processed for proximity ligation assay using antibodies to NS3 and GBF1. Stacks of images corresponding to the total volume of the cells were acquired, and maximum intensity projections of the stacks were generated. (C) Representative images. PLA signal (white dots) and nuclei (blue). (D) Quantification of dots of 12 images from 2 independent experiments. ***, $P < 0.001$.

this assay. This result indicated that GBF1 has a partial inhibitory action on the protease activity of NS3.

GBF1 interacts with NS3 in cells replicating HCV. Our data presented above indicated that NS3 interacts with GBF1 when expressed with NS4A. However, this interaction appeared to be reduced when NS3 was expressed as a part of the HCV polyprotein. To assess if NS3 interacts with GBF1 in HCV-replicating cells, we investigated the intracellular localization of both proteins in Huh-7 cells containing a subgenomic replicon. Interestingly, NS3 expression levels varied from cell to cell, and as in induced UNS3-4A-24 cells, the pattern of GBF1 staining was altered in cells expressing higher levels of NS3 (Fig. 6A). At higher magnification, the two proteins did not appear to be fully colocalized in the same structures. Rather, GBF1-containing vesicular structures were juxtaposed to NS3-containing membrane domains (Fig. 6B). We next performed a proximity ligation assay (PLA) in Huh-7 cells containing a subgenomic replicon

using NS3 and GBF1 antibodies. As a control, we also used naive Huh-7 cells. In naive cells, only very few fluorescent dots were observed, indicating that the antibodies yield a very low background when one interacting protein is absent (Fig. 6C). In replicon-containing cells, higher numbers of dots were observed. A signal-to-background ratio superior to 10 was calculated after quantification (Fig. 6D), indicating that a significant interaction occurred between NS3 and endogenous GBF1 in cells replicating HCV.

Isolation and characterization of NS3 mutants with reduced interaction to GBF1. To better characterize the interaction between NS3 and GBF1, we used a yeast two-hybrid-based approach to isolate mutants of the protease domain of NS3 with a reduced level of interaction with the Sec7 domain of GBF1. Mutations were introduced into NS3 by PCR-based random mutagenesis, and mutants were screened by reverse two-hybrid analysis to isolate yeast clones growing on nonselective medium but not on selective medium lacking histidine (−His). Growth on −His medium requires expression of the His3 reporter gene, which only occurs upon interaction of the two protein domains expressed in the yeast two-hybrid system. Out of 148 clones screened, 95 were selected using this reverse two-hybrid approach, 49 of which expressed an NS3 construct of the expected size in Western blot analysis. The pGBKT7-NS3 protease plasmids of these clones were isolated and sequenced. Eighteen clones had no mutation, 25 had one mutation, 5 had two mutations, and 1 clone had three mutations in the coding sequence of the NS3 protease domain. This led to the identification of 12 individual mutations, 4 double mutations, and 1 triple mutation, which inhibit NS3 protease-GBF1 Sec7 domain interaction (Fig. 7A).

We then focused on individual mutations. Mutated plasmids were reintroduced into yeast cells to confirm their phenotype. In contrast to the wild-type (WT) NS3 protease domain, all the mutants had a growth defect on selective medium (Fig. 7B). The localization of the mutated residues in the three-dimensional (3D) structure of the protease domain of NS3 was analyzed. Three residues, Asn-77, Cys-97, and Ile-114, are exposed at the surface of the protein (Fig. 7C), with calculated exposure of 20%, 15%, and 4%, respectively (the maximal exposure possible of a residue is approximately 63%). Structural changes resulting from mutations of surface residues could directly alter GBF1 interaction, whereas those involving buried residues may be transmitted to other parts of the protein and indirectly affect surface structure. Alternatively, mutation of internal residues may affect the folding of the domain and lead to a nonfunctional protein. Concerning surface-exposed residues, it is noteworthy that Cys-97 is implicated in Zn^{2+} coordination (44–46). Its mutation to Arg could lead to a loss of Zn^{2+} binding and to a major structural alteration of the protease domain. The two other residues, Asn-77 and Ile-114, are located on different faces of the domain (Fig. 7C). It is therefore unlikely that they could be part of a single interaction area.

Impact of NS3 mutations on viral replication. To assess the impact on genome replication of the mutations identified in the yeast two-hybrid assay, we introduced them into a Con1 replicon containing a luciferase reporter sequence (47). *In vitro*-transcribed replicon RNAs were electroporated into Huh-7.5 cells, and genome replication was assessed by measuring luciferase activity over a 96-h time course. The kinetics of replication of 4 mutants (V36A, L44Q, V107A, and I114T) was very similar to that of the WT replicon (Fig. 8A). The 8 other mutants behaved as the nonreplicative ΔGDD control and therefore were nonreplicative.

To test if the replicative mutants were affected in their interaction with GBF1, we analyzed their sensitivity to BFA. Replicon RNAs were electroporated into Huh-7.5 cells; electroporated cells were treated with BFA for 8 h and then cultured without BFA. The luciferase activity was measured at 48 h postelectroporation. The replication was inhibited by BFA in a dose-dependent manner (Fig. 8B). All mutants displayed a dose response very similar to that of the WT replicon, indicating that no alteration of BFA sensitivity was caused by any of the 4 mutations. All four mutants interacted with GBF1 in the coimmunoprecipitation assay (Fig. 8C). Taken together, these results suggest that no physical or functional alteration was provided by the mutations V36A, L44Q, V107A,

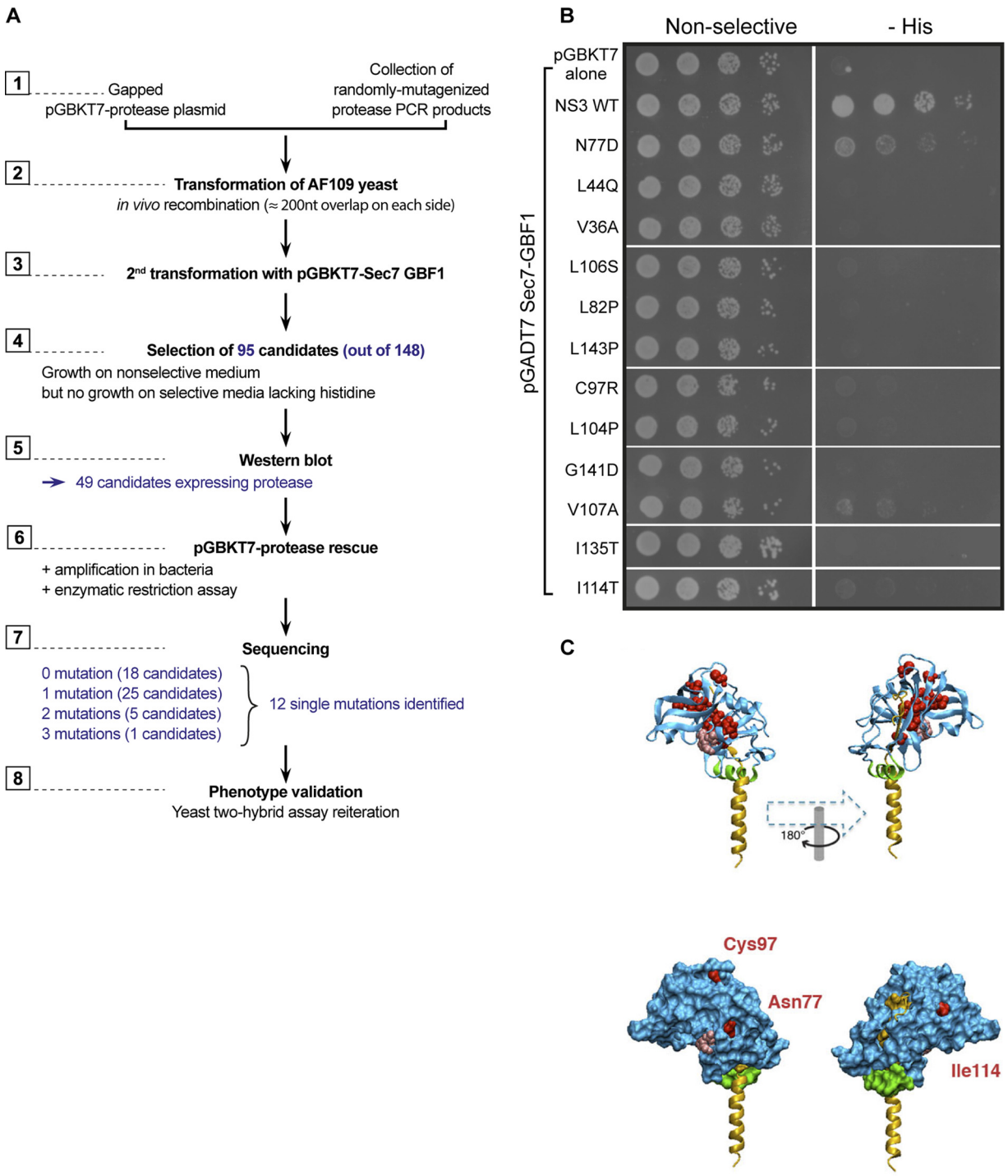

FIG 7 Interaction of Sec7-GBF1 with HCV NS3 protease mutants. (A) Protocol for selection of NS3 mutants that do not interact with GBF1 in the yeast two-hybrid assay. (B) Yeast strain AH109 cotransformed with pGADT7-Sec7-GBF1 and pGBKT7, carrying mutants of the NS3 protease domain, were grown on nonselective and selective (−His) media to monitor reporter expression. (B) Localization of mutated residues in the structure of the NS3 protease domain. Mutated residues are shown in red, NS3 active site is shown in pink, NS3 membrane-associated α-helix is in green, NS4A is in yellow, and other NS3 residues are in blue. Three residues mutated in the yeast reverse two-hybrid assay, which are exposed at the surface of the protein, are indicated.

and I114T concerning NS3-GBF1 interaction in a replicative model, in contrast to what had been observed in the yeast two-hybrid-based interaction assay. Some differences between the two interaction assays could result from the presence of the full-length protein combined with NS4A in the coimmunoprecipitation assay and of the protease domain only in the yeast two-hybrid assay.

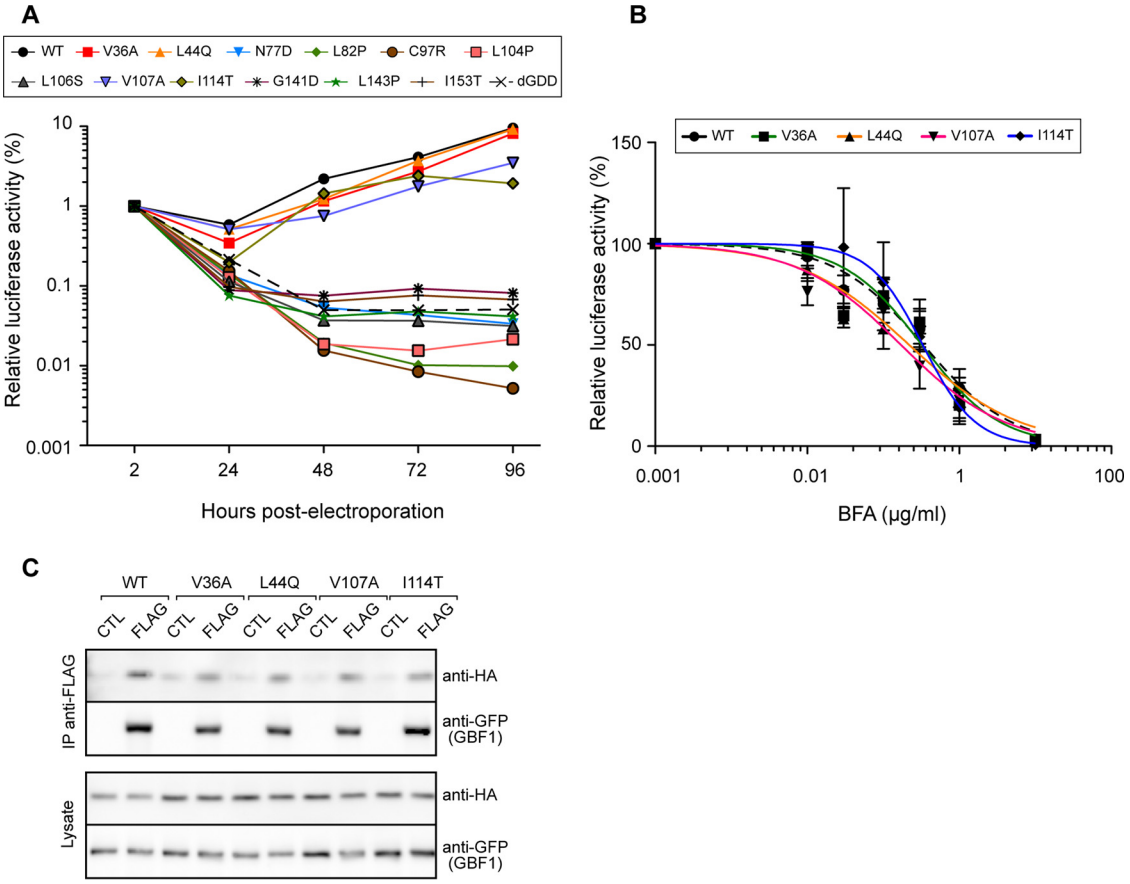

FIG 8 Replication and BFA sensitivity of NS3 protease domain mutants. (A) *In vitro*-transcribed RNA of Con1 replicon pFK-rep-PI-luc/ET containing NS3 protease mutants was electroporated into Huh-7.5 cells. Cells were lysed at the indicated times postelectroporation for luciferase assay. Data represent means from 4 independent experiments performed in triplicate. (B) Huh-7.5 cells electroporated with the indicated replicons were cultured for 8 h in the presence of the indicated concentrations of BFA and lysed at 48 h postelectroporation for luciferase assay. Luciferase activities were expressed relative to the luciferase activity measured at 2 h postelectroporation. Data are means from 3 independent experiments performed in triplicate. (C) WT HA-tagged NS3-4A or the indicated mutants were coexpressed with YFP-GBF1 (CTL) or YFP-GBF1-FLAG (FLAG) in HeLa cells. Cells were lysed and lysates precipitated with anti-FLAG beads. Immunoprecipitated material and 5% of lysates were analyzed by immunoblotting with anti-HA and anti-GFP antibodies.

Protease activity of NS3 mutants. To assess the protease activity of the mutants, we used the GFP-IPS cleavage assay. NS3 mutants were coexpressed with GFP-IPS in Huh-7 cells (Fig. 9A). For all replicative mutants, cleavage efficiency was very similar to that of the WT protease. Nonreplicative mutants yielded 3 phenotypes. L82P, C97R, G141D, and L143P appeared inactive, since no cleavage product was detected. For mutants L104P, L106S, and I153T, a partial cleavage was observed, suggesting that their protease activity was reduced. Finally, the protease activity of mutant N77D was similar to that of the WT and replicative mutants.

The expression levels of NS3 mutants were also monitored by immunoblotting (Fig. 9A). An expression similar to that of the WT was observed for all replicative mutants and for the nonreplicative, protease-active mutant N77D, reduced expression was observed for mutants L104P, L106S, and I153T, and no expression was observed for inactive mutants L82P, C97R, G141D, and L143P. We reasoned that reduced expression levels probably resulted from instability of the mutated proteins. To confirm this hypothesis, we treated transfected Huh-7 cells with MG132, a proteasome inhibitor, in order to inhibit the degradation of unstable proteins. As shown in Fig. 9B, MG132 treatment revealed the presence of a band migrating slightly slower than mature NS3 in lysates of cells transfected with inactive or partially active mutants. This band most probably represents uncleaved NS3-4A. This result suggests that mutations L82P, C97R, L104P, L106S, G141D, L131P, and I153T induced

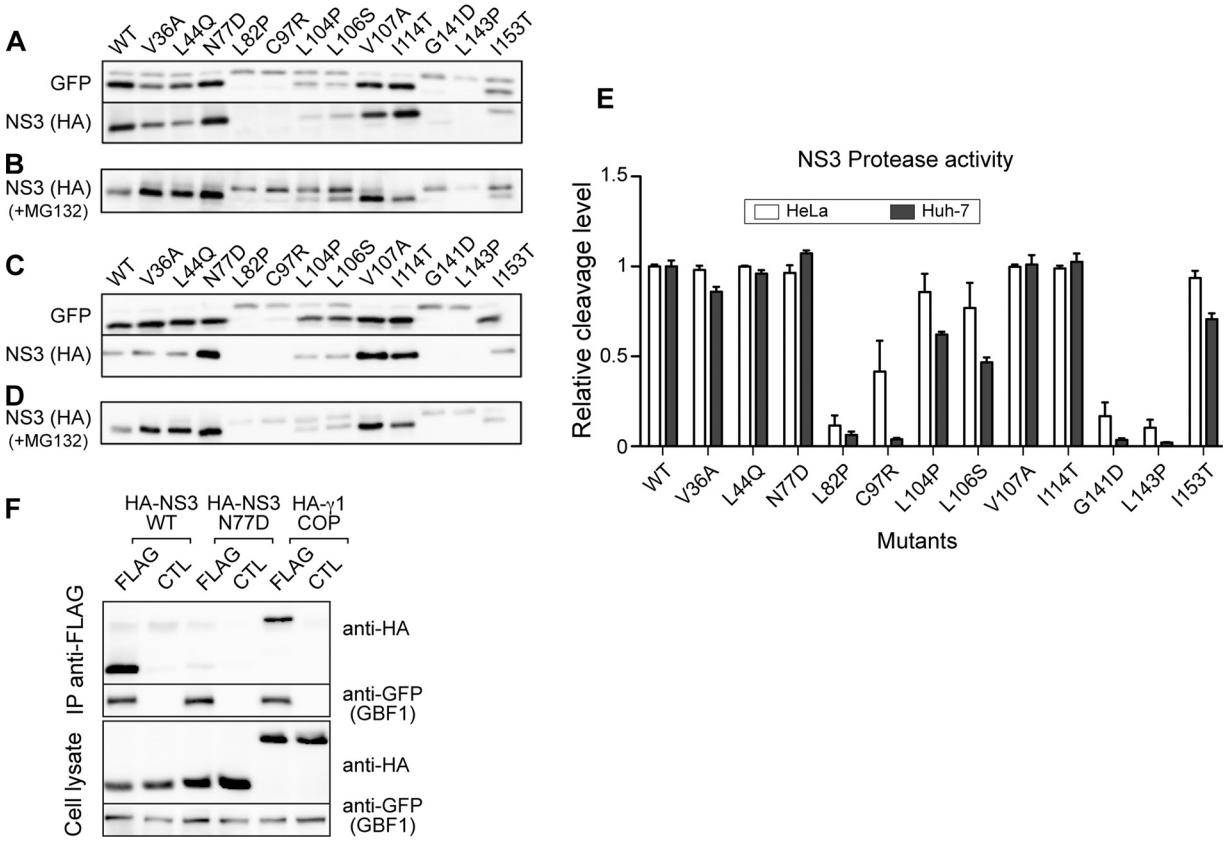

FIG 9 Protease activity of NS3 protease domain mutants. (A) GFP-IPS was expressed in Huh-7 cells with the indicated HA-tagged NS3-4A mutants. Cell lysates were analyzed by immunoblotting with anti-GFP and anti-HA antibodies. (B) Immunoblot analysis of Huh-7 cells expressing the indicated NS3-4A mutants and treated for 8 h with MG132. (C) Immunoblot analysis of GFP-IPS cleavage in HeLa cells. (D) Immunoblot analysis of NS3 in HeLa cells treated with MG132. (E) Quantification of GFP-IPS cleavage by NS3-4A mutants in Huh-7 and HeLa cells. Data are means and standard deviations from 3 independent experiments. (F) WT or S77D HA-tagged NS3-4A was coexpressed with YFP-GBF1 (CTL) or YFP-GBF1-FLAG (FLAG) in HeLa cells. Cells were lysed and lysates precipitated with anti-FLAG beads. Immunoprecipitated material and 5% of lysates were analyzed by immunoblotting with anti-HA and anti-GFP antibodies.

folding defects, which explain their reduced protease activity. Uncleaved NS3-4A was detected at much lower levels in cells expressing active proteases (WT, replicative mutants V36A, L44Q, V107A, and I114T, and nonreplicative mutant N77D), as expected for correctly folded proteins. It is noteworthy that the autoproteolytic cleavage efficiency (Fig. 9B) of mutated proteins correlated with the observed substrate cleavage efficiency (Fig. 9A) of the series of NS3 mutants.

We repeated these experiments in HeLa cells, which yield a higher level of expression of NS3. Again, mutants L82P, C97R, G141D, and L143P were inactive for both GFP-IPS cleavage (Fig. 9C) and autoproteolytic processing (Fig. 9D). Mutants L104P, L106S, and I153T were partially active, and mutants V36A, L44Q, N77D, V107A, and I114T appeared as active as the WT construct. The proteolytic cleavage of GFP-IPS in both cell lines was quantified (Fig. 9E). The results of this quantification showed a better proteolytic activity for partially active mutants in HeLa cells than in Huh-7 cells, in keeping with their higher expression levels in this cell line.

Altogether, the data indicate that NS3 protease domain mutants isolated using the yeast reverse two-hybrid screen include a series of 4 mutants (V36A, L44Q, V107A, and I114T), which are very similar to the WT concerning replication efficiency and proteolytic activity, a series of 7 mutants with reduced proteolytic activity (L82P, C97R, L104P, L106S, G141D, L143P, and I153T), which are not replicative, probably because of folding defects and/or reduced protease activity, and a mutant (N77D) that is not replicative despite having normal protease activity. The distinguishing features of the mutants are summarized in Table 1.

TABLE 1 Structural and functional properties of NS3 mutants

Position	Mutation (Con1)	Conservation[a]		Accessibility (%)	Replication	Protease activity	Self cleavage
		H77	JFH-1				
36	Val→Ala	Val	Ile	−	+	+	+
44	Leu→Gln	Leu	Leu	−	+	+	+
77	Asn→Asp	Asn	Ser	20	−	+	+
82	Leu→Pro	Leu	Leu	−	−	−	−
97	Cys→Arg	Cys	Cys	15	−	−	−
104	Leu→Pro	Leu	Leu	−	−	±	±
106	Leu→Ser	Leu	Leu	−	−	±	±
107	Val→Ala	Val	Val	−	+	+	+
114	Ile→Thr	Ile	Ile	4	+	+	+
141	Gly→Asp	Gly	Gly	−	−	−	−
143	Leu→Pro	Leu	Val	−	−	−	−
153	Ile→Thr	Leu	Leu	−	−	±	±

[a]+, similar to WT; −, not active, not replicative, or not accessible; ±, partially active.

To assess whether the lack of replication of mutant N77D correlates with an alteration of interaction of NS3 with GBF1 in human cells, we used the coimmunoprecipitation assay. A reduction of coimmunoprecipitated NS3 protein was observed with mutant N77D (Fig. 9F). This result confirmed that the N77D mutation altered the interaction between NS3 and GBF1.

The residue Ser77 of NS3 is important for JFH1 genome replication. We next investigated the phenotype of a mutation equivalent to N77D in the JFH-1 strain, which is much more replicative than Con1 in Huh-7 cells. At position 77, a Ser residue replaces in JFH-1 the Asn residue that is present in Con1 and H77 strains. The S77D mutation was introduced into a luciferase-expressing JFH-1 replicon and a replication assay was performed. Like mutant N77D of the Con1 strain, mutant S77D of the JFH-1 strain was not replicative (Fig. 10A). We also assessed the protease activity of mutant S77D using the GFP-IPS construct and observed no difference between WT and S77D cleavage efficiency (data not shown). These results indicated that the phenotypes of Con1 N77D and JFH-1 S77D mutants are similar.

To assess if mutation S77D alters interactions between NS3 and other viral proteins, we made use of the high replicative potential of the JFH-1 strain to try to obtain pseudorevertant mutant viruses that would rescue the phenotype of the S77D mutation. The S77D mutation was inserted into the full-length JFH-1 genome, and *in vitro*-transcribed RNA was introduced into Huh-7 cells by electroporation. As expected, we did not observe any HCV-positive cells at 3 days postelectroporation. However, after approximately 2 weeks of culture, a few positive cells began to appear and their number rose at each cell passage, indicating the presence of replicative viruses in the cell population. The experiment was done twice and each selection was done in duplicate. A similar kinetics of infectious virus generation was observed in each experiment. We sequenced the nonstructural protein-coding region of the viral genome. In one experiment, we found a reversion to a Ser residue at position 77 of NS3, which is the residue present in strain JFH-1. In the other experiment, the Asp77 residue was converted into an Asn residue, which is found at this position in other HCV strains. In this second experiment an additional mutation was found at position 221 of NS3, in the helicase domain, changing a Gln residue for a Leu residue. This Q221L mutation, which has been found previously in several studies (48–52), is a titer-enhancing mutation with no impact on replication. Therefore, it does not represent a pseudorevertant mutation that would reveal the presence of any potential interaction between protease and helicase domains of NS3. The mutations found in NS3 during these two experiments are recapitulated in Table 2. No other mutation was found in NS3, NS4A, NS4B, NS5A, and NS5B coding sequences in either experiment. Thus, we obtained no evidence that the mutation S77D could disrupt any interaction between NS3 protease and other nonstructural proteins of the viral replication complex.

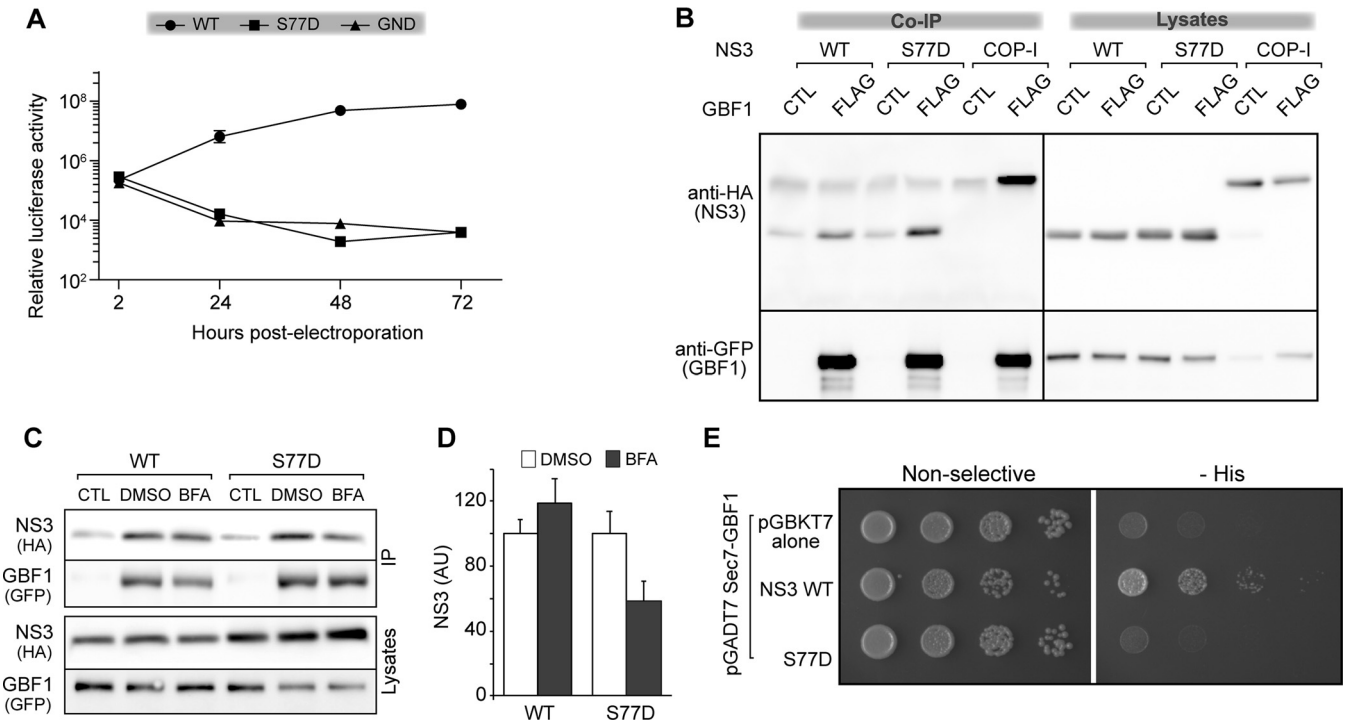

FIG 10 Phenotype of the S77D mutation in NS3 of strain JFH-1. *In vitro*-transcribed RNA of ΔE1E2 JFH-1 containing the indicated mutations was electroporated in Huh-7.5 cells. Cells were lysed at the indicated times postelectroporation and luciferase activity was measured. Data represent means from 3 independent experiments performed in triplicate. (B and C) HeLa cells were cotransfected with expression plasmids for HA-tagged WT or S77D NS3-4A or HA-tagged γ1-COP with YFP-GBF1 (CTL) or YFP-GBF1-FLAG (FLAG). Cells were left untreated (B) or were treated with 10 μg/ml BFA or 0.1% DMSO (C). Cells were lysed and lysates incubated with anti-FLAG beads. Immunoprecipitated material and 5% of lysates were analyzed by immunoblotting with anti-HA and anti-GFP antibodies. (D) NS3 signals from 4 independent experiments were quantified and normalized to values of DMSO-treated cells, which were expressed as 100. Errors bars represent SD. (E) Yeast strain AH109 cotransformed with pGADT7-Sec7-GBF1 and pGBKT7 carrying the WT or the N77D mutant of the NS3 protease domain were grown on nonselective and selective (−His) media to monitor reporter expression.

We next assessed the impact of the S77D mutation on the interaction between NS3 and GBF1 by coimmunoprecipitation. Surprisingly, mutated NS3 bound to GBF1 in this assay (Fig. 10B). S77D coimmunoprecipitation signal was similar to or slightly better than that of the WT. This could be explained by slightly higher expression levels of the mutated protein. We then investigated the impact of BFA on GBF1-NS3 interaction. Whereas no BFA effect on coimmunoprecipitation was observed for the WT, an ~50% decrease of the signal was observed for S77D (Fig. 10C and D), indicating that its interaction with GBF1 is more sensitive to BFA than that of the WT protein. This result suggests that the interaction between GBF1 and NS3 is altered by the mutation S77D. To further confirm this alteration of GBF1-NS3 interaction, we introduced the S77D mutation into the pGBKT7-NS3 plasmid and performed a yeast two-hybrid interaction assay. A reduction of interaction was observed for the mutant in this assay (Fig. 10E), confirming the impact of the mutation S77D on the GBF1-NS3 interaction.

DISCUSSION

In this study, we investigated GBF1 interactions with viral proteins during HCV infection. We found that GBF1 interacts with NS3. The GBF1-NS3 interaction was observed by yeast two-hybrid assay, by coimmunoprecipitation, and by GST pulldown,

TABLE 2 Mutations in NS3 of revertant viruses

Expt no.	Position	Mutation
1	77	Asp→Asn
	221	Gln→Leu
2	77	Asp→Ser

and the interaction between endogenous GBF1 and NS3 was also observed by proximity ligation assay in cells replicating HCV. Moreover, GBF1-NS3 interaction was also supported by the inhibition of NS3 protease activity by GBF1 and by the impact of NS3-4A expression on GBF1 intracellular localization. An alteration in the intracellular localization of GBF1 was observed both in inducible NS3-4A-expressing cells and in replicon-containing Huh-7 cells expressing higher levels of NS3, confirming the impact of NS3 on GBF1 intracellular localization in a more physiological model. This change in GBF1 intracellular localization is consistent with an alteration in Golgi structure, which has already been reported for HCV-infected cells (53–55). This change in Golgi morphology is due to the effects of HCV infection on GBF1 function (55). Importantly, we found that NS3-4A expression induced a change of GBF1 intracellular localization from Golgi membranes to NS3-positive structures and that this association with NS3-positive structures was insensitive to BFA, indicating that it was independent of Arf activation. All of these observations are consistent with the existence of a physical and functional interaction between NS3 and GBF1.

This interaction of GBF1 with NS3 is consistent with the crucial role of GBF1 at the onset of genome replication, since the NS3-4A protease mediates one of the earliest steps of HCV replication, the proteolytic processing of the polyprotein. Therefore, NS3 is well placed to interact with host factors implicated at the onset of genome replication. The GBF1-NS3 interaction appears to be reduced when other viral proteins are coexpressed, as suggested by experiments using inducible cells and by moderate signals obtained in the proximity ligation assay with replicon-containing cells. GBF1 is not a component of mature HCV replication complexes, and its inhibition has a limited impact on HCV genome replication once the replication is established (14). In contrast, its inhibition during early times of the replication period strongly inhibits HCV infection. This suggests that GBF1 fulfills an essential function during the onset of genome replication that is not required later during the HCV life cycle. For other viruses, a similar involvement of GBF1 early during genome replication has also been reported. Much like for HCV, BFA inhibits the replication of dengue virus and mouse hepatitis coronavirus (MHV) when the cells are treated just after virus entry, but the inhibition is less important when BFA is added later (24, 25). During MHV infection, GBF1 transiently colocalizes with replication complexes early in infection (24). These data suggest that GBF1 acts at an early step of genome replication of these viruses, as for HCV. During poliovirus infection, GBF1 is also recruited early to RNA replication sites. However, in this case, the colocalization is still visible at later time points (56), in line with the existence of differences of GBF1 involvement in HCV and poliovirus replication (33, 57).

HCV genome replication includes a latent period of 16 to 20 h in Huh-7 cells, during which viral protein synthesis occurs at levels that are undetectable by immunofluorescence. Kinetics experiments indicated that GBF1 function is crucial for HCV replication during this period. Therefore, it is not possible to experimentally verify if a transient recruitment of GBF1 to nascent replication complexes actually occurs when its function is essential for genome replication. Later during HCV infection, when replication complexes become detectable by immunofluorescence, no GBF1 recruitment was observed (14), consistent with the limited functional importance of GBF1 for HCV replication at this time. Therefore, we can only speculate that the NS3-GBF1 interaction participates in the function of GBF1 in genome replication during the latent period.

We observed that NS3-4A inhibited protein secretion weakly and only at higher expression levels. Therefore, it is unlikely that NS3 would have any impact on the regulatory role of GBF1 in the secretory pathway during HCV infection, particularly during early steps of genome replication, when NS3 expression levels are likely very limited. On the other hand, we observed an inhibition of NS3 protease activity by GBF1. This modulation of NS3-4A protease activity might help in genome replication by facilitating the generation of the polyprotein. Additionally, NS3-GBF1 interaction might be important for recruiting GBF1 or some of its effectors to specific intracellular locations. Further work will be required to test these possibilities.

The interaction was mapped to the protease domain of NS3 and the Sec7 domain

of GBF1. An Asn or Ser residue at position 77, located on the surface of the protease domain, appears to be part of the interaction region. Its replacement by an Asp residue in Con1 and JFH-1 strains strongly inhibits genome replication without altering NS3 protease activity. Although we cannot exclude that this mutation could also disrupt interactions with other viral and/or host proteins, in addition to GBF1, the reduced interaction observed in yeast two-hybrid and coimmunoprecipitation assays for the Con1 strain strongly suggests that the interaction with GBF1 is indeed altered, suggesting that the lack of replication of the mutant virus could result from a lack of interaction between GBF1 and NS3. The lack of pseudorevertant virus isolation argues against the Asp77 mutation disrupting interaction of NS3 with any other viral protein.

Interactions between GBF1 and viral proteins have been reported for other GBF1-dependent viruses. GBF1 interacts with nonstructural protein NS5 of dengue virus; however, the interaction domains were not mapped (25). GBF1 also interacts with nonstructural protein 3A of two enteroviruses, poliovirus and coxsackievirus B3 (58). In contrast to HCV NS3, the interaction with 3A was not mapped to the Sec7 domain but to the N-terminal part of GBF1, upstream of the Sec7 domain (59). The difference of interacting domains correlates with a difference of function of GBF1 during HCV and enterovirus genome replication. GBF1 function in poliovirus infection does not require the Sec7 domain and therefore does not depend on the ArfGEF activity of GBF1 but rather requires the N terminus of GBF1 that interacts with poliovirus 3A (57). In contrast, HCV genome replication is not supported by the N-terminal region of GBF1 and requires its ArfGEF activity within the Sec7 domain. More precisely, GBF1 function during HCV infection is mediated by the pair of class II Arfs, Arf4 and Arf5, but not by Arf1 (33). Therefore, it is likely that GBF1 function during HCV genome replication involves the regulation of specific, not yet identified effectors of Arf4 and/or Arf5. We recently reported that class II Arfs are also important for other GBF1-dependent RNA viruses from different families but not for the enterovirus coxsackievirus B4 (35), again emphasizing the difference of GBF1 function during enterovirus and HCV genome replication. Therefore, positive-sense single-stranded RNA viruses appear to have evolved different strategies for using different functions of GBF1. HCV and other viruses of the families *Flaviviridae* and possibly *Coronaviridae* would require the ArfGEF activity of GBF1 to activate class II Arfs, whereas enteroviruses appear to use an ArfGEF-independent function of GBF1. Interestingly, both of these functions are different from the well-documented function of GBF1 in the regulation of the early secretory pathway, which depends on its ArfGEF activity but is mediated by another pair of Arfs, Arf1 and Arf4 (33, 34). The future identification of effectors of class II Arfs implicated in viral replication might open the way to defining novel mechanisms of action of GBF1. Their identification could also lead to developing new antiviral therapies.

MATERIALS AND METHODS

Reagents. Dulbecco's modified Eagle's medium (DMEM), phosphate-buffered saline (PBS), goat and fetal calf sera (FCS), and 4′,6-diamidino-2-phenylindole (DAPI) were purchased from Life Technologies. 3-Amino-1,2,4-triazole (3-AT) was from MP Biomedicals. Protease inhibitor mix (Complete) was from Roche. Other chemicals were from Sigma-Aldrich.

Antibodies. Mouse anti-NS3 monoclonal antibody (MAb) 1848 was from Virostat. Mouse anti-NS5A MAb 9E10 was kindly provided by C. M. Rice, the Rockefeller University, NY, USA. Rabbit anti-GBF1 serum 9D4 was kindly provided by P. Melançon, University of Alberta, AB, Canada. Mouse anti-GBF1 MAb was from BD Biosciences. Mouse anti-GFP MAb and rat anti-HA MAb 3F10 were from Roche. Peroxidase-conjugated goat anti-mouse IgG and goat anti-rat IgG were from Jackson Immunoresearch. Alexa 647-conjugated goat anti-mouse IgG and Alexa 555-conjugated goat anti-rabbit IgG were from Molecular Probes.

DNA constructs. HCV NS3 of strains H77 and Con1 (full-length proteins and protease and helicase domains) were cloned into pGBKT7 using NdeI and BamHI sites. HCV NS3 of strain JFH-1 (full-length protein and protease domain, both wild type and S77D) were cloned into pGBKT7 using EcoRI and BamHI sites. HCV NS3 helicase of strain JFH-1 was cloned into pGBKT7 using NcoI and BamHI sites.

Plasmids for the cell culture-adapted Con1 replicon, named pFK-rep-PI-luc/ET (originally designated pFK-nt341-sp-PI-lucEI3420-9605/5.1), and the corresponding GDD mutant (47) were kindly provided by Ralf Bartenschlager (University of Heidelberg, Germany). V36A, L44Q, N77D, L82P, C97R, L104P, L106S, V107A, and I114T mutations were inserted by transferring HindIII-MreI from the corresponding pGBKT7 plasmids into pFKi-rep-PI-Luc/ET plasmid. Mutations G141D, L143P, and I153T were inserted by site-

directed mutagenesis. All mutagenized fragments were verified by sequencing. The JFH-1 construct used for the replication assay (HCVcc-Rluc/ΔE1E2) was previously described (14). The mutation S77D was introduced by PCR-based site-directed mutagenesis.

pEYFP-GBF1 was described previously (42). To construct pEYFP-GBF1-FLAG, used in coimmunoprecipitation experiments, the coding sequence of a FLAG tag was inserted between the last codon of GBF1 and the stop codon. To generate expression plasmids for HA-tagged NS3-4A of the Con1 strain, the coding sequence of the protease domain was amplified from pGBKT7 plasmids using primers 5′-CTAG AGGATCCATGGCGCCTATTACGGCCTAC-3′ and 5′-GAAGACCGGTGACCGCATAG-3′. The coding sequence of NS3 helicase domain and NS4A was amplified from pFK-rep-PI-luc/ET using primers 5′-CTATGCGGT CACCGGTCTTC-3′ and 5′-CGACGAATTCTTAGCACTCTTCCATCTCATCGA-3′. Both PCR products were fused using external primers and inserted into pcDNA3.1-HA using BamHI and EcoRI sites. The HA-tagged γ1-COP construct was previously described (36).

The expression plasmid used to express the NS3 substrate GFP-IPS was generated in two steps. First, oligonucleotides 5′-AGCTTCACCAAAAAAAAAAAGAAAAGTAGGAGG-3′ and 5′-GATCCCTCCTACTTTTCTTT TTTTTTTTGGTGA-3′ were phosphorylated, annealed, and ligated into HindIII- and BamHI-restricted pEGFP-C1 to generate pEGFP-NLS. The coding sequence of the IPS C-terminus next was amplified by PCR with oligonucleotides 5′-AGTTATCTAGACTAGTGCAGACGCCGCCGGTACA-3′and 5′-TCCGAGGGCACCTTT GGGAT-3′. The PCR product was inserted into the BamHI-XbaI sites of pEGFP-NLS.

The coding sequence of the protease domain of NS3 (Con1 strain) was amplified by PCR using primers 5′-TACGCTTCTAGAGGATCCATGGCGCC-3′ and 5′-GTCGACGAATTCTTACCGCATAGTGGTTTCCATA GA-3′ and introduced into the pGEX4T-1 plasmid to create the pGEX4T-1-pro plasmid using the restriction sites BamHI and EcoRI.

Yeast two-hybrid. Yeast two-hybrid analysis was performed in *Saccharomyces cerevisiae* strain AH109 (Clontech). Coding sequences for GBF1, BIG1, and BIG2 full-length proteins or domains were cloned into pGADT7, creating Gal4 activation domain fusion proteins. pGBKT7 plasmids carrying HCV genes, to produce Gal4 DNA binding domain fusion proteins, were a kind gift of Hyo-Young Chung and Charles Rice (Rockefeller University, New York, USA). These pGBKT7 plasmids contained each viral protein cloned from a Jc1 HCV genome that is a fusion of J6 and JFH-1 HCV genomes. The junction point of this J6-JFH-1 hybrid viral sequence is located in NS2. Thus, the sequences were the following: J6-Core, E1, E2, and p7; Jc1-NS2 and JFH-1-NS3, NS4A, NS4B, NS5A, and NS5B. HCV NS3 protease or helicase domain-coding sequences were also cloned into pGBKT7 (this study). pGADT7 and pGBKT7 fusion constructs were transformed into yeast by the lithium acetate method using carrier DNA and plated on nonselective plates (lacking leucine and tryptophan) to select for the two yeast two-hybrid plasmids. After growth, the colonies were transferred to selective plates (lacking histidine) to assay expression of the reporter HIS3 gene, which only occurs if the fusion proteins interact.

Random mutagenesis, reverse two-hybrid assay, and plasmid rescue. Mutagenic PCR was performed with 0.5 μl of pGBKT7-protease (Con1 strain) plasmid using 0.5 μl of *Taq* DNA polymerase (New England Biolabs) in a 50-μl reaction mixture containing 200 nM primer 5′- GGTCTCCGCTGACTAG GGCACATCTGACAGAAGTG–3′, 200 nM primer 5′-CCGGTAGAGGTGTGGTCAATAAGAGCGACCTCATGC-3′, and 200 μM each deoxynucleoside triphosphate (dNTP). Samples were placed at 95°C for 5 min and then with cycling parameters set to 95°C for 30 s, 65°C for 2.5 min, and 72°C for 2 min for 30 cycles, and then incubation at 72°C for 5 min. In parallel, gapped plasmid was produced by enzymatic restriction of pGBKT7-protease (Con1 strain) plasmid using NdeI and BamHI sites. Both mutagenic PCR product and gapped plasmid were gel purified using a QIAquick gel extraction kit (Qiagen) according to the manufacturer's protocol. They were transformed into AH109 yeast by the lithium acetate method using carrier DNA and plated on nonselective plates lacking tryptophan. After growth, transformants were pooled, transformed with pGADT7-Sec7GBF1, and plated on selective plates lacking leucine and tryptophan to select for the presence of the two plasmids. After growth, the colonies were transferred to His3 reporter expression selective plates (lacking histidine). Plasmids were rescued from yeast using a NucleoSpin plasmid miniprep kit (Macheray-Nagel). Yeast cells resuspended in buffer A1 were disrupted by agitation with glass beads. Glass beads were removed by centrifugation. Lysis and plasmid isolation were performed according to the manufacturer's protocol. Plasmids were subsequently transformed into bacteria and purified using a NucleoSpin plasmid miniprep kit according to the manufacturer's protocol.

Cell culture. Huh-7 cells (60) and Huh-7.5 cells (61) were grown in Dulbecco's modified Eagle's medium (DMEM), high-glucose modification, supplemented with GlutaMAX I and 10% FCS. UNS3-4A-24 (38), UNS5Acon-6 (39), and UHCV-11 (40) cells were kindly provided by D. Moradpour (University of Lausanne, Switzerland). They were grown in DMEM supplemented with 10% FCS, 1 μg/ml puromycin (Gibco), 0.4 mg/ml G418 (PAA), and 1 μg/ml tetracycline (Sigma-Aldrich). HeLa cells were provided by B. Goud (Institut Curie, Paris, France). They were grown in minimal Eagle's medium alpha supplemented with GlutaMAX I and 10% FCS. All cell lines were grown at 37°C with 5% CO_2.

UNS3-4A-24, UNS5Acon6, and UHCV-11 cell induction. One day before induction, cells were plated on glass coverslips in a medium containing 0.1 μg/ml tetracycline. For induction, cells were rinsed three times with PBS to remove tetracycline and cultured for 24 h in tetracycline-free medium. Control noninduced cells were cultured for 24 h in the presence of 1 μg/ml tetracycline.

Immunofluorescence microscopy. For immunofluorescence microscopy, cells were grown on glass coverslips and fixed with 4% formaldehyde (Sigma-Aldrich) for 5 min on ice, followed by 20 min at room temperature. All subsequent steps were realized at room temperature. Cells were permeabilized by a 1-h incubation in blocking buffer (2% BSA, 0.5% saponin [Sigma-Aldrich, St. Louis, MO, USA] in PBS). Both primary and secondary antibody incubations were carried out in blocking buffer for 1 h and 45 min, respectively. Nuclei were stained by a 5-min incubation in PBS containing 1 μg/ml DAPI. Coverslips were

mounted on glass slides using Prolong antifade gold (Invitrogen), sealed, and stored at 4°C. Images were acquired using an inverted laser scanning confocal microscope (TCS SP5 AOBS tandem; Leica). Signals were sequentially collected by using single fluorescence excitation and acquisition settings to avoid crossover. Images were assembled by using Image J software.

Colocalization was evaluated using the plugin JACoP of ImageJ (62). The extent of colocalization of GBF1 and NS3 was measured with Pearson's coefficient, which is a correlation coefficient describing the relationship between the intensities in two images. For each cell analyzed, a region of interest was manually defined. The pixels corresponding to the background were removed from the analysis using the automatic method of Costes included in the JACoP plugin, and the foreground pixels were used to calculate the Pearson's coefficient.

Replication assay. Huh-7.5 cells were electroporated with HCVcc-Rluc/ΔE1E2 or rep-PI-luc/ET *in vitro*-transcribed RNA and seeded in 24-well plates. The luciferase activity was measured 2 h (Con1), 4 h (JFH-1), 24 h, 48 h, 72 h, and 96 h postelectroporation using the *Renilla* luciferase assay system kit from Promega.

NS3-4A protease assay. Twenty-four hours before transfection, HeLa or Huh-7 cells were seeded in 24-well clusters to reach ~70% confluence the next day. For assessing the protease activity of mutants, cells were cotransfected with 125 ng of pcDNA3.1 HA-NS3-4A and 125 ng of pEGFP-IPS mixed with Trans-IT LT1 reagent by following the instructions of the manufacturer (Mirus). For assessing the impact of NS3 expression on secretion, cells were cotransfected with 100 ng of pEGFP-IPS and 15 ng of pcDNA3.1 HA-NS3-4A and increasing concentrations of GBF1 (50, 100, 200, and 300 ng). Empty pcDNA3.1 plasmid was used to keep the same final concentration of total transfected DNA. At 24 h posttransfection, EGFP-IPS and NS3 expression were monitored by immunoblotting using anti-GFP and anti-HA antibodies, respectively.

Immunoblotting. Cells were rinsed 3 times with cold PBS and lysed at 4°C for 20 min in a buffer containing 50 mM Tris-Cl, pH 7.5, 100 mM NaCl, 2 mM EDTA, 1% Triton X-100, 0.1% SDS, 1 mM phenylmethylsulfonyl fluoride (PMSF), and a mix of protease inhibitors (Complete). Insoluble material was removed by centrifugation at 4°C. The protein content was determined by the bicinchoninic acid method as recommended by the manufacturer (Sigma), using bovine serum albumin as the standard. The proteins were then resolved by SDS-PAGE and transferred onto nitrocellulose membranes (Hybond-ECL; Amersham) using a Trans-Blot apparatus (Bio-Rad). Proteins of interest were revealed with specific primary antibodies, followed by species-specific secondary antibodies conjugated to peroxidase. Proteins were visualized using enhanced chemiluminescence (ECL Plus; GE Healthcare). The signals were recorded using a LAS 3000 apparatus (Fujifilm). Quantification of unsaturated signals was carried out using the gel quantification function of ImageJ.

Coimmunoprecipitation. HeLa cells were seeded in 6-well clusters the day before transfection and were cotransfected with 750 ng of pcDNA3.1 HA-NS3-4A and 750 ng of pEYFP-GBF1 or pEYFP-GBF1-FLAG using the Trans-IT LT1 reagent as recommended by the manufacturer (Mirus). At 40 h posttransfection, cells were rinsed 3 times with cold PBS and lysed in 400 μl of a solution containing 50 mM Tris-Cl, pH 7.4, 100 mM NaCl, 0.5% Triton X-100, and protease inhibitors at 4°C. Insoluble material was removed by centrifugation at 4°C. Twenty μl of lysate was removed for immunoblot analysis. Lysates were rotated at 4°C for 4 h with 30 μl of anti-FLAG M2 affinity agarose gel (from Sigma-Aldrich), previously rinsed twice with 1 ml of lysis solution. Beads were washed 3 times with the lysis solution, and immunoprecipitated material was eluted by incubating the beads with 30 μl of SDS-PAGE loading buffer at 70°C for 10 to 15 min. Proteins of lysates and immunoprecipitations were quantified by immunoblotting using anti-GFP (GBF1) and anti-HA (NS3) antibodies.

Proximity ligation assay. Naïve and replicon (JFH-1)-containing Huh-7 cells cultured on glass coverslips were fixed with 3% paraformaldehyde for 20 min, rinsed with PBS, and permeabilized in PBS containing 0.1% Triton X-100 for 5 min. Proximity ligation assay was performed using Duolink *in situ* detection kit DUO92007 (Sigma), as recommended by the manufacturer, with mouse anti-NS3 MAb 486D39 (provided by J. F. Delagneau, Bio-Rad) and rabbit anti-GBF1 affinity-purified antiserum (ab86701; Abcam), both diluted to 1:100. Images were acquired using a laser-scanning confocal microscope (LSM880; Zeiss) using a 63× oil immersion objective with a 1.4 numerical aperture. For each field, a stack of images corresponding to the total volume of the cells was acquired. Maximum-intensity projection images were generated using Zen software. Representative images were assembled and dots were counted using ImageJ software. For each field, the mean number of spots per cell was calculated by dividing the number of spots by the number of nuclei.

GST pulldown. Recombinant GST-pro fusion protein and GST were purified from *Escherichia coli* BL21(DE3)/pLysS harboring the plasmids pGEX4T-1-pro and pGEX4T-1, respectively. Five hundred ml of cells was grown in LB medium containing 100 μg/ml ampicillin until the optical density at 600 nm (OD_{600}) was approximately 0.6, and the expression of the proteins was induced by adding 0.1 mM isopropyl-β-D-thiogalactopyranoside for 2 h at 30°C. Cells were pelleted and stored at −80°C until used. Cells pellets were thawed and resuspended into 10 ml of lysis buffer (50 mM Tris-Cl, pH 8.8, 100 mM NaCl, 5 mM EDTA, 15% sucrose) containing Complete protease inhibitors (Roche), 1 mM PMSF, and 10 μg/ml bovine pancreatic DNase I (Sigma-Aldrich). Cells were lysed using a French press and centrifuged for 20 min at 20,000 × *g* to remove insoluble material. The lysate was incubated for 2 h at room temperature with 1 ml of equilibrated glutathione-Sepharose 4B beads (GE Healthcare) previously equilibrated with 50 mM Tris-Cl, pH 8.0. The beads were then transferred to a column and washed extensively with 50 mM Tris-Cl, pH 8.0. Recombinant proteins were eluted 2 times with 1 ml of 50 mM Tris-Cl, pH 8.0, containing 20 mM reduced glutathione and 0.1 mM dithiothreitol and dialyzed against 50 mM Tris-Cl, pH 8.0. The purity of the proteins was verified by SDS-PAGE and

Coomassie blue staining. The OD_{280} values of the dialyzed protein solutions were measured and their concentrations calculated using the absorption coefficients and molecular masses computed using the ProtParam tool (Expasy).

Secretion assay. Twenty-four hours before transfection, HeLa cells were seeded in 24-well clusters to reach ~70% confluence the next day. Cells were cotransfected with 25 ng pCMV-GLuc (New England Biolabs) and increasing amounts of pcDNA3.1-HA-NS3-4A (JFH1) (100, 200, and 300 ng) mixed with Trans-IT LT1 reagent by following the instructions of the manufacturer (Mirus). The total amount of DNA was kept constant by adding empty pcDNA3.1. At 16 h posttransfection, the culture medium was changed, and the cells were incubated for 4 h. As a control, cells transfected with 25 ng pCMV-GLuc and 300 ng pcDNA3.1 were treated with 1 μg/ml BFA during this 4-h secretion period. Luciferase activity was measured in the supernatant and cell lysates using a Renilla luciferase assay system kit from Promega as recommended by the manufacturer.

SUPPLEMENTAL MATERIAL

Supplemental material for this article may be found at https://doi.org/10.1128/JVI.01459-18.

SUPPLEMENTAL FILE 1, XLSX file, 0.01 MB.

ACKNOWLEDGMENTS

We thank C. M. Rice, P. Melançon, R. Bartenschlager, D. Moradpour, and J.-F. Delagneau for kindly providing us with invaluable reagents, F. Penin for help with the localization of mutated residues in the structure of the NS3 protease domain, and S. Belouzard for the GFP-IPS construct. We thank M.-P. Golinelli, C. Guyot, M. Le Provost, and A. Yu for excellent technical assistance and S. Ung for help in assembling figures.

This work was supported in part by the French Agence Nationale de Recherche sur le Sida et les Hépatites Virales (ANRS). L.G. was supported by a postdoctoral fellowship from ANRS.

REFERENCES

1. Gosert R, Egger D, Lohmann V, Bartenschlager R, Blum HE, Bienz K, Moradpour D. 2003. Identification of the hepatitis C virus RNA replication complex in Huh-7 cells harboring subgenomic replicons. J Virol 77:5487–5492. https://doi.org/10.1128/JVI.77.9.5487-5492.2003.
2. Ferraris P, Blanchard E, Roingeard P. 2010. Ultrastructural and biochemical analyses of hepatitis C virus-associated host cell membranes. J Gen Virol 91:2230–2237. https://doi.org/10.1099/vir.0.022186-0.
3. Romero-Brey I, Merz A, Chiramel A, Lee JY, Chlanda P, Haselman U, Santarella-Mellwig R, Habermann A, Hoppe S, Kallis S, Walther P, Antony C, Krijnse-Locker J, Bartenschlager R. 2012. Three-dimensional architecture and biogenesis of membrane structures associated with hepatitis C virus replication. PLoS Pathog 8:e1003056. https://doi.org/10.1371/journal.ppat.1003056.
4. Egger D, Wölk B, Gosert R, Bianchi L, Blum HE, Moradpour D, Bienz K. 2002. Expression of hepatitis C virus proteins induces distinct membrane alterations including a candidate viral replication complex. J Virol 76:5974–5984. https://doi.org/10.1128/JVI.76.12.5974-5984.2002.
5. Gao L, Aizaki H, He J-W, Lai MMC. 2004. Interactions between viral nonstructural proteins and host protein hVAP-33 mediate the formation of hepatitis C virus RNA replication complex on lipid raft. J Virol 78:3480–3488. https://doi.org/10.1128/JVI.78.7.3480-3488.2004.
6. Reiss S, Rebhan I, Backes P, Romero-Brey I, Erfle H, Matula P, Kaderali L, Poenisch M, Blankenburg H, Hiet M-S, Longerich T, Diehl S, Ramirez F, Balla T, Rohr K, Kaul A, Bühler S, Pepperkok R, Lengauer T, Albrecht M, Eils R, Schirmacher P, Lohmann V, Bartenschlager R. 2011. Recruitment and activation of a lipid kinase by hepatitis C virus NS5A is essential for integrity of the membranous replication compartment. Cell Host Microbe 9:32–45. https://doi.org/10.1016/j.chom.2010.12.002.
7. Tai AW, Salloum S. 2011. The role of the phosphatidylinositol 4-kinase PI4KA in hepatitis C virus-induced host membrane rearrangement. PLoS One 6:e26300. https://doi.org/10.1371/journal.pone.0026300.
8. Berger KL, Kelly SM, Jordan TX, Tartell MA, Randall G. 2011. Hepatitis C virus stimulates the phosphatidylinositol 4-kinase III alpha-dependent phosphatidylinositol 4-phosphate production that is essential for its replication. J Virol 85:8870–8883. https://doi.org/10.1128/JVI.00059-11.
9. Bianco A, Reghellin V, Donnici L, Fenu S, Alvarez R, Baruffa C, Peri F, Pagani M, Abrignani S, Neddermann P, De Francesco R. 2012. Metabolism of phosphatidylinositol 4-kinase IIIα-dependent PI4P is subverted by HCV and is targeted by a 4-anilino quinazoline with antiviral activity. PLoS Pathog 8:e1002576. https://doi.org/10.1371/journal.ppat.1002576.
10. Reiss S, Harak C, Romero-Brey I, Radujkovic D, Klein R, Ruggieri A, Rebhan I, Bartenschlager R, Lohmann V. 2013. The lipid kinase phosphatidylinositol-4 kinase III alpha regulates the phosphorylation status of hepatitis C virus NS5A. PLoS Pathog 9:e1003359. https://doi.org/10.1371/journal.ppat.1003359.
11. Stone M, Jia S, Heo WD, Meyer T, Konan KV. 2007. Participation of rab5, an early endosome protein, in hepatitis C virus RNA replication machinery. J Virol 81:4551–4563. https://doi.org/10.1128/JVI.01366-06.
12. Wang H, Perry JW, Lauring AS, Neddermann P, De Francesco R, Tai AW. 2014. Oxysterol-binding protein is a phosphatidylinositol 4-kinase effector required for HCV replication membrane integrity and cholesterol trafficking. Gastroenterology 146:1373–1385. https://doi.org/10.1053/j.gastro.2014.02.002.
13. Khan I, Katikaneni DS, Han Q, Sanchez-Felipe L, Hanada K, Ambrose RL, Mackenzie JM, Konan KV. 2014. Modulation of hepatitis C virus genome replication by glycosphingolipids and FAPP2 protein. J Virol 88:12276–12295. https://doi.org/10.1128/JVI.00970-14.
14. Goueslain L, Alsaleh K, Horellou P, Roingeard P, Descamps V, Duverlie G, Ciczora Y, Wychowski C, Dubuisson J, Rouillé Y. 2010. Identification of GBF1 as a cellular factor required for hepatitis C virus RNA replication. J Virol 84:773–787. https://doi.org/10.1128/JVI.01190-09.
15. Claude A, Zhao BP, Kuziemsky CE, Dahan S, Berger SJ, Yan JP, Armold AD, Sullivan EM, Melançon P. 1999. GBF1: a novel Golgi-associated BFA-resistant guanine nucleotide exchange factor that displays specificity for ADP-ribosylation factor 5. J Cell Biol 146:71–84.
16. Donaldson JG, Jackson CL. 2011. ARF family G proteins and their regulators: roles in membrane transport, development and disease. Nat Rev Mol Cell Biol 12:362–375. https://doi.org/10.1038/nrm3117.
17. Wright J, Kahn RA, Sztul E. 2014. Regulating the large Sec7 ARF guanine nucleotide exchange factors: the when, where and how of activation. Cell Mol Life Sci 71:3419–3438. https://doi.org/10.1007/s00018-014-1602-7.
18. Bui QT, Golinelli-Cohen M-P, Jackson CL. 2009. Large Arf1 guanine nucleotide exchange factors: evolution, domain structure, and roles in membrane trafficking and human disease. Mol Genet Genomics 282:329–350. https://doi.org/10.1007/s00438-009-0473-3.

19. Szul T, Grabski R, Lyons S, Morohashi Y, Shestopal S, Lowe M, Sztul E. 2007. Dissecting the role of the ARF guanine nucleotide exchange factor GBF1 in Golgi biogenesis and protein trafficking. J Cell Sci 120:3929–3940. https://doi.org/10.1242/jcs.010769.
20. Bouvet S, Golinelli-Cohen M-P, Contremoulins V, Jackson CL. 2013. Targeting of the Arf-GEF GBF1 to lipid droplets and Golgi membranes. J Cell Sci 126:4794–4805. https://doi.org/10.1242/jcs.134254.
21. Belov GA, Feng Q, Nikovics K, Jackson CL, Ehrenfeld E. 2008. A critical role of a cellular membrane traffic protein in poliovirus RNA replication. PLoS Pathog 4:e1000216. https://doi.org/10.1371/journal.ppat.1000216.
22. Lanke KHW, van der Schaar HM, Belov GA, Feng Q, Duijsings D, Jackson CL, Ehrenfeld E, van Kuppeveld FJM. 2009. GBF1, a guanine nucleotide exchange factor for Arf, is crucial for coxsackievirus B3 RNA replication. J Virol 83:11940–11949. https://doi.org/10.1128/JVI.01244-09.
23. Wang J, Du J, Jin Q. 2014. Class I ADP-ribosylation factors are involved in enterovirus 71 replication. PLoS One 9:e99768. https://doi.org/10.1371/journal.pone.0099768.
24. Verheije MH, Raaben M, Mari M, Lintelo Te EG, Reggiori F, van Kuppeveld FJM, Rottier PJM, de Haan CAM. 2008. Mouse hepatitis coronavirus RNA replication depends on GBF1-mediated ARF1 activation. PLoS Pathog 4:e1000088. https://doi.org/10.1371/journal.ppat.1000088.
25. Carpp LN, Rogers RS, Moritz RL, Aitchison JD. 2014. Quantitative proteomic analysis of host-virus interactions reveals a role for Golgi brefeldin A resistance factor 1 (GBF1) in dengue infection. Mol Cell Proteomics 13:2836–2854. https://doi.org/10.1074/mcp.M114.038984.
26. Farhat R, Ankavay M, Lebsir N, Gouttenoire J, Jackson CL, Wychowski C, Moradpour D, Dubuisson J, Rouillé Y, Cocquerel L. 7 November 2017. Identification of GBF1 as a cellular factor required for hepatitis E virus RNA replication. Cell Microbiol. https://doi.org/10.1111/cmi.12804.
27. Zhang L, Hong Z, Lin W, Shao R-X, Goto K, Hsu VW, Chung RT. 2012. ARF1 and GBF1 generate a PI4P-enriched environment supportive of hepatitis C virus replication. PLoS One 7:e32135. https://doi.org/10.1371/journal.pone.0032135.
28. Tai AW, Benita Y, Peng LF, Kim S-S, Sakamoto N, Xavier RJ, Chung RT. 2009. A functional genomic screen identifies cellular cofactors of hepatitis C virus replication. Cell Host Microbe 5:298–307. https://doi.org/10.1016/j.chom.2009.02.001.
29. Vaillancourt FH, Pilote L, Cartier M, Lippens J, Liuzzi M, Bethell RC, Cordingley MG, Kukolj G. 2009. Identification of a lipid kinase as a host factor involved in hepatitis C virus RNA replication. Virology 387:5–10. https://doi.org/10.1016/j.virol.2009.02.039.
30. Berger KL, Cooper JD, Heaton NS, Yoon R, Oakland TE, Jordan TX, Mateu G, Grakoui A, Randall G. 2009. Roles for endocytic trafficking and phosphatidylinositol 4-kinase III alpha in hepatitis C virus replication. Proc Natl Acad Sci U S A 106:7577–7582. https://doi.org/10.1073/pnas.0902693106.
31. Borawski J, Troke P, Puyang X, Gibaja V, Zhao S, Mickanin C, Leighton-Davies J, Wilson CJ, Myer V, Cornellataracido I, Baryza J, Tallarico J, Joberty G, Bantscheff M, Schirle M, Bouwmeester T, Mathy JE, Lin K, Compton T, Labow M, Wiedmann B, Gaither LA. 2009. Class III phosphatidylinositol 4-kinase alpha and beta are novel host factor regulators of hepatitis C virus replication. J Virol 83:10058–10074. https://doi.org/10.1128/JVI.02418-08.
32. Trotard M, Lepère-Douard C, Régeard M, Piquet-Pellorce C, Lavillette D, Cosset F-L, Gripon P, Le Seyec J. 2009. Kinases required in hepatitis C virus entry and replication highlighted by small interference RNA screening. FASEB J 23:3780–3789. https://doi.org/10.1096/fj.09-131920.
33. Farhat R, Séron K, Ferlin J, Fénéant L, Belouzard S, Goueslain L, Jackson CL, Dubuisson J, Rouillé Y. 2016. Identification of class II ADP-ribosylation factors as cellular factors required for hepatitis C virus replication. Cell Microbiol 18:1121–1133. https://doi.org/10.1111/cmi.12572.
34. Volpicelli-Daley LA, Li Y, Zhang C-J, Kahn RA. 2005. Isoform-selective effects of the depletion of ADP-ribosylation factors 1-5 on membrane traffic. Mol Biol Cell 16:4495–4508. https://doi.org/10.1091/mbc.e04-12-1042.
35. Ferlin J, Farhat R, Belouzard S, Cocquerel L, Bertin A, Hober D, Dubuisson J, Rouillé Y. 2018. Investigation of the role of GBF1 in the replication of positive-sense single-stranded RNA viruses. J Gen Virol 99:1086–1096. https://doi.org/10.1099/jgv.0.001099.
36. Deng Y, Golinelli-Cohen M-P, Smirnova E, Jackson CL. 2009. A COPI coat subunit interacts directly with an early-Golgi localized Arf exchange factor. EMBO Rep 10:58–64. https://doi.org/10.1038/embor.2008.221.
37. Schmidt-Mende J, Bieck E, Hügle T, Penin F, Rice CM, Blum HE, Moradpour D. 2001. Determinants for membrane association of the hepatitis C virus RNA-dependent RNA polymerase. J Biol Chem 276:44052–44063. https://doi.org/10.1074/jbc.M103358200.
38. Wolk B, Sansonno D, Kräusslich HG, Dammacco F, Rice CM, Blum HE, Moradpour D. 2000. Subcellular localization, stability, and trans-cleavage competence of the hepatitis C virus NS3-NS4A complex expressed in tetracycline-regulated cell lines. J Virol 74:2293–2304. https://doi.org/10.1128/JVI.74.5.2293-2304.2000.
39. Brass V, Bieck E, Montserret R, Wölk B, Hellings JA, Blum HE, Penin F, Moradpour D. 2002. An amino-terminal amphipathic alpha-helix mediates membrane association of the hepatitis C virus nonstructural protein 5A. J Biol Chem 277:8130–8139. https://doi.org/10.1074/jbc.M111289200.
40. Moradpour D, Kary P, Rice CM, Blum HE. 1998. Continuous human cell lines inducibly expressing hepatitis C virus structural and nonstructural proteins. Hepatology 28:192–201. https://doi.org/10.1002/hep.510280125.
41. Klausner RD, Donaldson JG, Lippincott-Schwartz J. 1992. Brefeldin A: insights into the control of membrane traffic and organelle structure. J Cell Biol 116:1071–1080. https://doi.org/10.1083/jcb.116.5.1071.
42. Niu T-K, Pfeifer AC, Lippincott-Schwartz J, Jackson CL. 2005. Dynamics of GBF1, a brefeldin A-sensitive Arf1 exchange factor at the Golgi. Mol Biol Cell 16:1213–1222. https://doi.org/10.1091/mbc.e04-07-0599.
43. Jones CT, Catanese MT, Law LMJ, Khetani SR, Syder AJ, Ploss A, Oh TS, Schoggins JW, Macdonald MR, Bhatia SN, Rice CM. 2010. Real-time imaging of hepatitis C virus infection using a fluorescent cell-based reporter system. Nat Biotechnol 28:167–171. https://doi.org/10.1038/nbt.1604.
44. Love RA, Parge HE, Wickersham JA, Hostomsky Z, Habuka N, Moomaw EW, Adachi T, Hostomska Z. 1996. The crystal structure of hepatitis C virus NS3 proteinase reveals a trypsin-like fold and a structural zinc binding site. Cell 87:331–342. https://doi.org/10.1016/S0092-8674(00)81350-1.
45. Kim JL, Morgenstern KA, Lin C, Fox T, Dwyer MD, Landro JA, Chambers SP, Markland W, Lepre CA, O'Malley ET, Harbeson SL, Rice CM, Murcko MA, Caron PR, Thomson JA. 1996. Crystal structure of the hepatitis C virus NS3 protease domain complexed with a synthetic NS4A cofactor peptide. Cell 87:343–355. https://doi.org/10.1016/S0092-8674(00)81351-3.
46. Stempniak M, Hostomska Z, Nodes BR, Hostomsky Z. 1997. The NS3 proteinase domain of hepatitis C virus is a zinc-containing enzyme. J Virol 71:2881–2886.
47. Lohmann V, Hoffmann S, Herian U, Penin F, Bartenschlager R. 2003. Viral and cellular determinants of hepatitis C virus RNA replication in cell culture. J Virol 77:3007–3019. https://doi.org/10.1128/JVI.77.5.3007-3019.2003.
48. Yi M, Ma Y, Yates J, Lemon SM. 2007. Compensatory mutations in E1, p7, NS2, and NS3 enhance yields of cell culture-infectious intergenotypic chimeric hepatitis C virus. J Virol 81:629–638. https://doi.org/10.1128/JVI.01890-06.
49. Ma Y, Yates J, Liang Y, Lemon SM, Yi M. 2008. NS3 helicase domains involved in infectious intracellular hepatitis C virus particle assembly. J Virol 82:7624–7639. https://doi.org/10.1128/JVI.00724-08.
50. Phan T, Beran RKF, Peters C, Lorenz IC, Lindenbach BD. 2009. Hepatitis C virus NS2 protein contributes to virus particle assembly via opposing epistatic interactions with the E1-E2 glycoprotein and NS3-NS4A enzyme complexes. J Virol 83:8379–8395. https://doi.org/10.1128/JVI.00891-09.
51. Counihan NA, Rawlinson SM, Lindenbach BD. 2011. Trafficking of hepatitis C virus core protein during virus particle assembly. PLoS Pathog 7:e1002302. https://doi.org/10.1371/journal.ppat.1002302.
52. Chatel-Chaix L, Germain M-A, Motorina A, Bonneil É, Thibault P, Baril M, Lamarre D. 2013. A host YB-1 ribonucleoprotein complex is hijacked by hepatitis C virus for the control of NS3-dependent particle production. J Virol 87:11704–11720. https://doi.org/10.1128/JVI.01474-13.
53. Jones DM, Atoom AM, Zhang X, Kottilil S, Russell RS. 2011. A genetic interaction between the core and NS3 proteins of hepatitis C virus is essential for production of infectious virus. J Virol 85:12351–12361. https://doi.org/10.1128/JVI.05313-11.
54. Bishé B, Syed GH, Field SJ, Siddiqui A. 2012. Role of phosphatidylinositol 4-phosphate (PI4P) and its binding protein GOLPH3 in hepatitis C virus secretion. J Biol Chem 287:27637–27647. https://doi.org/10.1074/jbc.M112.346569.
55. Hansen MD, Johnsen IB, Stiberg KA, Sherstova T, Wakita T, Richard GM, Kandasamy RK, Meurs EF, Anthonsen MW. 2017. Hepatitis C virus triggers Golgi fragmentation and autophagy through the immunity-related GTPase M. Proc Natl Acad Sci U S A 114:E3462–E3471. https://doi.org/10.1073/pnas.1616683114.
56. Richards AL, Soares-Martins JAP, Riddell GT, Jackson WT. 2014. Genera-

tion of unique poliovirus RNA replication organelles. mBio 5:e00833-13. https://doi.org/10.1128/mBio.00833-13.
57. Belov GA, Kovtunovych G, Jackson CL, Ehrenfeld E. 2010. Poliovirus replication requires the N-terminus but not the catalytic Sec7 domain of ArfGEF GBF1. Cell Microbiol 12:1463–1479. https://doi.org/10.1111/j.1462-5822.2010.01482.x.
58. Wessels E, Duijsings D, Niu T-K, Neumann S, Oorschot VM, de Lange F, Lanke KHW, Klumperman J, Henke A, Jackson CL, Melchers WJG, van Kuppeveld FJM. 2006. A viral protein that blocks Arf1-mediated COP-I assembly by inhibiting the guanine nucleotide exchange factor GBF1. Dev Cell 11:191–201. https://doi.org/10.1016/j.devcel.2006.06.005.
59. Wessels E, Duijsings D, Lanke KHW, Melchers WJG, Jackson CL, van Kuppeveld FJM. 2007. Molecular determinants of the interaction between coxsackievirus protein 3A and guanine nucleotide exchange factor GBF1. J Virol 81:5238–5245. https://doi.org/10.1128/JVI.02680-06.
60. Nakabayashi H, Taketa K, Miyano K, Yamane T, Sato J. 1982. Growth of human hepatoma cells lines with differentiated functions in chemically defined medium. Cancer Res 42:3858–3863.
61. Lindenbach BD, Evans MJ, Syder AJ, Wölk B, Tellinghuisen TL, Liu CC, Maruyama T, Hynes RO, Burton DR, McKeating JA, Rice CM. 2005. Complete replication of hepatitis C virus in cell culture. Science 309:623–626. https://doi.org/10.1126/science.1114016.
62. Bolte S, Cordelières FP. 2006. A guided tour into subcellular colocalization analysis in light microscopy. J Microsc 224:213–232. https://doi.org/10.1111/j.1365-2818.2006.01706.x.